



ISTITUTO NAZIONALE DI RICERCA METROLOGICA Repository Istituzionale

Microbial consortia inoculants differently shape ecophysiological and systemic defence responses of field-grown grapevine cuttings

Original

Microbial consortia inoculants differently shape ecophysiological and systemic defence responses of field-grown grapevine cuttings / Sandrini, Marco; Chitarra, Walter; Pagliarani, Chiara; Moffa, Loredana; Petrozziello, Maurizio; Colla, Paola; Velasco, Riccardo; Balestrini, Raffaella; Nerva, Luca. - In: PLANT STRESS. - ISSN 2667-064X. - 14:(2024). [10.1016/j.stress.2024.100686]

Availability:

This version is available at: 11696/82359 since: 2024-12-02T18:03:05Z

Publisher:

Elsevier B.V.

Published

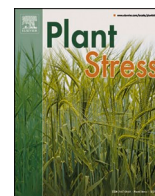
DOI:10.1016/j.stress.2024.100686

Terms of use:

This article is made available under terms and conditions as specified in the corresponding bibliographic description in the repository

Publisher copyright

(Article begins on next page)



Microbial consortia inoculants differently shape ecophysiological and systemic defence responses of field-grown grapevine cuttings[☆]

Marco Sandrini^{a,b,1}, Walter Chitarra^{a,c,1,*}, Chiara Pagliarani^c, Loredana Moffa^a,
Maurizio Petrozziello^a, Paola Colla^d, Riccardo Velasco^a, Raffaella Balestrini^e, Luca Nerva^{a,c,*}

^a Council for Agricultural Research and Economics, Research Centre for Viticulture and Enology (CREA-VE), Via XXVIII Aprile 26, 31015 Conegliano (TV), Italy

^b University of Udine, Department of Agricultural, Food, Environmental and Animal Sciences, Via delle Scienze 206, 33100, Udine (UD), Italy

^c National Research Council of Italy - Institute for Sustainable Plant Protection (IPSP-CNR), Strada delle Cacce 73, 10135 Torino (TO), Italy

^d Istituto Nazionale di Ricerca Metrologica (INRiM), Strada delle Cacce 91, 10135 Torino (TO), Italy

^e National Research Council of Italy, Institute of Biosciences and Bioresources (IBBR), Via Giovanni Amendola 165/A, 70126 Bari (BA), Italy

ARTICLE INFO

Keywords:

Plant-microbe interaction
Gas exchange
Grapevine
AMF
Endophyte
Actinomycetes

ABSTRACT

Despite microbe-based products for grapevine protection and growth improvement are available, only a few of them contain microbes directly isolated from vine tissues. Here, a collection of endophytic bacterial isolates obtained from grapevine woody tissues was used for producing an *ad-hoc* inoculum. Bacterial isolates were tested in biocontrol assays against some of the main grapevine pathogens and the seven most performing as biological control agents were selected for a consortium development (SynCom). Before putting them in field, a group of cuttings was inoculated with the developed SynCom, whereas a second one was inoculated with a commercial consortium formed by a mixed inoculum of arbuscular mycorrhizal fungi (AMF) and a rhizosphere *Bacillus coagulans* bacterial strain (B). After the transplanting in field, eco-physiological parameters were monitored, and samples for biochemical and molecular analyses were collected at the end of the experiment. Integration of physiological data with metabolite and transcriptome profiles have been performed. Results showed that the SynCom slowed down photosynthesis, suggesting a reallocation of energy towards defence pathways. Conversely, the AMF+B treatment led to more balanced physiological performances. Metabarcoding analysis revealed that SynCom-treated plants had a significantly lower abundance of wood-decay pathogens than control or AMF+B plants. Collectively, our findings provide information useful for enabling microbial inoculation exploitation with a refined awareness.

1. Introduction

Plants naturally share their environment with a multitude of microbes, some of which can colonize their inner tissues becoming endophytes, strongly influencing plant life cycle and responses to environmental stimuli (Nerva et al., 2022d). The recruitment of microbes by plants (*i.e.*, microbiome assembly) strictly depends on the interaction between plants and the surrounding environment and, once the relationship is established, the plant and its microbiome behave as a unique super organism, referred to as a holobiont (Vandenkoornhuysen et al., 2015). Based on the global climate change scenarios and increased

frequency of stressful biotic and abiotic events, the development of novel, sustainable crop protection strategies is extremely urgent to improve agricultural resilience (Chitarra et al., 2015; Giudice et al., 2021, 2022). In this context, a better understanding of plant-microbe interactions could help to dissect key factors involved in the recruitment of beneficial microbes by the host (Jurburg et al., 2022; Nerva et al., 2022d). The great advances in microbial biotechnology and metagenomics, as well as in the collections of microbes, provide an available treasure to manipulate bacterial communities on a large scale (Zou et al., 2019; Sandrini et al., 2022a). It is in fact possible to cultivate pure strains, characterize them and develop synthetic microbial

[☆] This article is part of a special issue entitled: "Impact of climate change in viticulture: understanding and mitigating abiotic and biotic stress in grapevine" published at the journal *Plant Stress*.

* Corresponding authors at: CREA - Research Centre for Viticulture and Enology (CREA-VE), Via XXVIII Aprile, 26, 31015 Conegliano (TV), Italy.

E-mail addresses: walter.chitarra@crea.gov.it (W. Chitarra), luca.nerva@crea.gov.it (L. Nerva).

¹ These authors equally contributed to this work.

communities (SynComs) to mimic natural microbiome functions. The application of multi- and interdisciplinary approaches allows to study its effects on plant performances upon diverse environmental conditions (Trivedi et al., 2020; Sandrini et al., 2022b). Interestingly, the assembly rules for establishing plant microbiota have been revealed in gnotobiotic *Arabidopsis* plants using a drop-out and late introduction approach with SynComs composed of sixty-two native strains. The authors found that community assembly has historical contingency with priority effects and a certain degree of resistance to late microbe arrivals (Carlström et al., 2019). These findings provided new insights into plant-microbiome interactions and suggested that, to be successful, application of SynComs should be performed at the early stages of the host life cycle, when the plant-associated microbial community is still under development.

Several beneficial endophytes-inhabiting plant tissues (e.g., Plant Growth-Promoting microorganisms, such as *Actinomycetes*, and Arbuscular Mycorrhizal Fungi, AMF) play key roles in protecting plants against biotic and abiotic stresses (Chitarra et al., 2016; Carrión et al., 2019; Sandrini et al., 2022a; Gul et al., 2023; Fiorilli et al., 2024; Kavaya et al., 2024). During the last decade, diverse approaches based on the use of rhizosphere microbial microorganisms, including the application of SynComs, have been reported in the literature, highlighting the increased attention on this subject for orienting future sustainable agricultural practices (Sandrini et al., 2022a).

Plant diseases cause significant losses in agricultural production that lead not only to decreased yields and quality, but also to biodiversity loss, mitigation costs due to control measures, with important downstream impacts on human health (Ristaino et al., 2021). Once infected by pathogens, plants react promptly by activating endogenous defence responses that are tightly mediated by phytohormones such as jasmonic acid (JA), ethylene (Et) and salicylic acid (SA). These phytochemicals orchestrate several signaling pathways from cells to systemic routes by means of the so-called systemic acquired resistance (SAR, mediated by SA) or induced systemic resistance (ISR, mediated by JA and Et) (Burketova et al., 2015). The last can be activated either following pathogen attacks or by beneficial soil-inhabiting microbes (e.g., Plant Growth Promoting Bacteria - PGPB, AMF) recruited by plants thanks to the modulation of signaling through the root exudates abundantly released under stressful conditions (Berendsen et al., 2018; Williams and de Vries, 2020). The development of tailored SynComs could represent a powerful tool to prime plants against biotic (and/or abiotic) stresses (Qiu et al., 2019). A simplified SynCom formed by three bacterial species was able to synergistically protect *Arabidopsis* plants against downy mildew (Berendsen et al., 2018). Another study, using a SynCom composed of thirty-eight bacterial strains (Lebeis, 2015), demonstrated that immune signaling is the driver of microbiome development in *Arabidopsis*. Recently, Li et al. (2021) assembled two SynComs (one complex and another simplified with a community of four species) with disease controlling functions against *Fusarium* sp., i.e., the causal agent of root rot disease in *Astragalus mongholicus*. These authors observed that both SynComs were successful in controlling the disease development via synergistic cooperation by activating ISR paths in the host. The native microbiome is continuously modulated based on the host genotype and environmental stimuli. Similarly, SynCom structure and functionality can be strongly influenced by the same variables. A deep understanding of SynCom functionality in “natural” environments would improve their potential to be fully exploited (Wei et al., 2018; Veach et al., 2019), especially considering that several of the available studies were conducted in axenic conditions.

Grapevine (*Vitis vinifera*) is one of the most economically significant fruit crops worldwide, primarily cultivated for wine and table grape production, but also for other products such as distillates, juice, raisins, vinegar, jelly, seed oil, and extracts. In 2020, the global grape production reached 80 million tons, making grapevine the third most economically valuable horticultural crop, with an estimated farm-gate value near to 70 billion US dollars. These economic factors, along with extensive scientific research across various fields—from genomics

to vineyard management practices and the characterization of wine and table grapevine traits—have led *Vitis vinifera* to be recognized as a model woody crop species (Gambetta et al., 2020; Keller, 2020; Khandani et al., 2024; van Leeuwen et al., 2024). Grapevine plants are challenged by many pathogens (mainly fungi or fungi-like) both in pre- and post-harvest (e.g., powdery and downy mildews, grey mold, esca syndrome). Their impact is strongly influenced by climate changes, with current projections indicating that disease incidence and severity will increase in Northern Italy and many other European wine regions in the near future (van Leeuwen et al., 2024). These pathogens, which cause significant quality and yield losses, are usually controlled by massive pesticide applications. However, the chemical approach strongly impacts the vineyard ecosystem, beneficial microbiota and human health, making the development of new sustainable alternatives extremely urgent (Armijo et al., 2016; Nerva et al., 2019; Giudice et al., 2022; Nerva et al., 2022b). Currently, microbial-based products for grapevine defence are still limited on the market, and studies on novel inoculants are poor. Research efforts evaluating their real effectiveness are therefore pivotal to deepen this subject. To this aim, beside experimental trials performed under controlled conditions, tests conducted in open-field systems, where environmental factors can greatly influence plant-microbe interactions, are needed (Basile et al., 2020).

In this study, we investigated whether root inoculation with a simplified SynCom formed by potential biocontrol agents could activate constitutive defence responses in the host able to modulate whole plant physiological responses to the surrounding environment. In detail, a SynCom consortium formed by seven bacterial isolates retrieved from the inner grapevine woody tissues (Nerva et al., 2022a) was developed and inoculated in grapevine rooted cuttings prior to planting them in the open field. The developed consortium was compared with a commercial one, formed by a mixed inoculum of a rhizospheric bacterial strain and different AMF species, reported as a biofertilizer able to induce stress tolerance. As previously mentioned, AMF can also prime plants against biotic stress through a mechanism known as Mycorrhiza-Induced Resistance (MIR). This has been observed in several crops, including grapevine, where a substantial accumulation of defense-related metabolites (such as stilbenoids) occurs within plant tissues, even in natural conditions (Nerva et al., 2022b; Nerva et al., 2023). To this end, combined ecophysiological, biochemical and molecular approaches were used to compare the developed SynCom and the commercial AMF-based inoculum effects on the host physiological performances and ISR activation. The implementation of consortia development protocols for future scale-up and field applications will be also discussed.

2. Material and methods

2.1. Culture-dependent approach to isolate grape bacterial endophytes

To ensure the capability to stably colonize grape tissues, cultivable pure bacteria were isolated from the inner woody tissue of field-grown *Vitis vinifera* plants as previously reported (Nerva et al., 2022a) and stored at the CREA – Research Centre for Viticulture and Enology microbial bank (<https://www.revine-prima2020.org/vimed>). Briefly, fresh woody tissue was ground and resuspended in water amended with 0.1% Sodium Dodecyl Sulfate (SDS). The tissue with the water was vortexed for at least 45 minutes, diluted 1:5 with water and plated on sodium propionate medium (SPM) (Jiang et al., 2016; Nerva et al., 2022a). Fifteen days after plating, colonies were isolated using sterile needles and the bacterial colonies moved onto CYA media. After total genomic DNA extractions, forty-four isolates were identified using the 16S sequence amplification (universal 27F 5'-AGAGTTTGATCCTGGCTCAG-3' and 1392R 5'-GGTTACCTTGTACGACTT-3') and sequenced by the Sanger method at BioFab Research srl (Italy). A search for similar sequences was conducted with the BLASTn tool (Basic Local Alignment Tool) on the GeneBank database, as reported in Table 1.

Table 1

Biological control activity of the whole bacterial collection. Data for biological control activity are referred to the pathogen growth inhibition rate (%) towards each fungal pathogen. The reported values of pathogen growth inhibition rate are the mean values of three replicates \pm SD for each isolate. The selected isolates forming the SynCom are reported in bold.

| Code | Phylum | Specific epithet | <i>B. cinerea</i> Pathogen Growth Inhibition Rate (%) | <i>P. minimum</i> | <i>N. parvum</i> | <i>G. bidwellii</i> |
|---------------|-----------------------|--|--|----------------------------------|----------------------------------|---------------------------------|
| ACT1 | Actinobacteria | <i>Micromonospora</i> sp. | - | - | - | 27.9 \pm 3.25 |
| ACT2 | Actinobacteria | <i>Actinomadura glauciflava</i> | 17.85\pm0.10 | 26.15\pm0.10 | - | 49.6\pm1.77 |
| ACT3 | Actinobacteria | <i>Saccharopolyspora</i> sp. | 16.42 \pm 0.10 | 7.69 \pm 0.10 | - | 12.1 \pm 1.06 |
| ACT4 | Actinobacteria | <i>Actinomadura glauciflava</i> | 16.67 \pm 0.10 | 28.92 \pm 1.50 | - | 42.1 \pm 3.18 |
| ACT5 | Actinobacteria | <i>Kocuria palustris</i> | - | - | - | 18.3 \pm 0.71 |
| ACT6 | Actinobacteria | <i>Micrococcus</i> sp. | - | - | - | 7.1 \pm 0.35 |
| ACT7 | Proteobacteria | <i>Methylobacterium</i> sp. | - | 7.69 \pm 0.10 | - | 55.4 \pm 0.71 |
| ACT8 | - | Uncultured | 7.35 \pm 2.48 | - | - | 32.9 \pm 2.47 |
| ACT9 | Actinobacteria | <i>Rhodococcus</i> sp. | - | 22.46 \pm 1.00 | - | 46.7 \pm 3.54 |
| ACT10 | Actinobacteria | <i>Mycobacterium hodleri</i> | - | - | - | 57.5 \pm 3.01 |
| ACT11 | Actinobacteria | <i>Nocardioides</i> sp. | - | - | - | 21.3 \pm 3.28 |
| ACT12 | Actinobacteria | <i>Asanoa</i> sp. | 96.43\pm0.10 | 16.92\pm0.10 | - | 56.7\pm2.50 |
| ACT13 | Actinobacteria | <i>Plantibacter</i> sp. | - | - | - | 59.6 \pm 0.35 |
| ACT15 | Actinobacteria | <i>Methylobacterium</i> sp. | 4.17 \pm 0.71 | 45.54 \pm 1.00 | - | 29.7 \pm 0.35 |
| ACT16 | Actinobacteria | <i>Cellulomonas</i> sp. | 25.88 \pm 1.41 | - | - | - |
| ACT17 | Actinobacteria | <i>Nocardioides cavernae</i> | 10.00 \pm 4.24 | - | - | 65 \pm 1.41 |
| ACT18 | Proteobacteria | <i>Pseudomonas</i> sp. | 96.43 \pm 0.10 | 10.46 \pm 0.50 | - | 11.7 \pm 0.71 |
| ACT19 | Proteobacteria | <i>Methylobacterium adhaesivum</i> | - | 7.69 \pm 0.10 | - | 44.6 \pm 0.35 |
| ACT20 | Unidentified | - | - | 3.64 \pm 0.50 | - | 63.3 \pm 0.71 |
| ACT21 | Proteobacteria | <i>Methylobacterium adhaesivum</i> | - | - | - | 42.5 \pm 2.12 |
| ACT22 | Proteobacteria | <i>Methylobacterium tardum</i> | - | 8.62 \pm 0.50 | - | 41.3 \pm 3.18 |
| ACT23 | Proteobacteria | <i>Methylorubrum extorquens</i> | - | 1.23 \pm 0.50 | - | 24.6 \pm 3.50 |
| ACT24 | Actinobacteria | <i>Nocardioides</i> sp. | - | 16 \pm 0.50 | - | 30 \pm 0.71 |
| ACT25 | Proteobacteria | <i>Rhizobium</i> sp. | 25.29\pm0.71 | 11.82\pm0.10 | - | 61.3\pm0.35 |
| ACT26 | Proteobacteria | <i>Methylobacterium adhaesivum</i> | - | - | - | 42.1 \pm 1.06 |
| ACT27 | Proteobacteria | <i>Methylobacterium</i> sp. | 25.89 \pm 0.71 | - | - | 44.6 \pm 0.35 |
| ACT28 | Proteobacteria | <i>Rhizobium</i> sp. | - | 44.62 \pm 0.10 | - | 37.5 \pm 0.71 |
| ACT29 | Proteobacteria | <i>Methylobacterium</i> sp. | - | - | - | 27.9 \pm 2.47 |
| ACT30 | Actinobacteria | <i>Nocardia</i> sp. | - | 24.31 \pm 1.00 | - | - |
| ACT31 | Actinobacteria | <i>Nocardioides</i> sp. | 95.29 \pm 1.41 | - | 11.76 \pm 3.50 | 15.8 \pm 0.71 |
| ACT32 | Actinobacteria | <i>Streptosporangium</i> sp. | - | - | - | - |
| ACT33 | Proteobacteria | <i>Rhizobium</i> sp. | - | 14.15 \pm 1.50 | - | 69.2 \pm 2.12 |
| ACT35 | Proteobacteria | <i>Methylobacterium radiotolerans</i> | 96.43\pm0.10 | 1.23\pm1.50 | - | 49.6\pm0.35 |
| ACT36 | Actinobacteria | <i>Mycobacterium</i> sp. | 35.71 \pm 0.10 | 2.15 \pm 1.50 | - | 77.9 \pm 1.06 |
| ACT37 | Proteobacteria | <i>Methylopila oligotropha</i> | - | - | - | 24.2 \pm 3.00 |
| ACT38 | Actinobacteria | <i>Microbacterium</i> sp. | - | 21.54 \pm 1.00 | - | 41.3 \pm 1.77 |
| ACT39 | Proteobacteria | <i>Agrobacterium</i> sp. | 1.47 \pm 1.77 | - | - | 50 \pm 0.00 |
| ACT40 | Actinobacteria | <i>Microbacterium</i> sp. | - | - | - | 11.7 \pm 0.00 |
| ACT41 | Actinobacteria | <i>Micrococcus yunnanensis</i> | 2.06 \pm 1.06 | - | - | 25.4 \pm 3.18 |
| AR1 | Proteobacteria | <i>Pseudomonas psychrotolerans</i> | 94.04 \pm 0.10 | 19.55 \pm 1.77 | - | 24.6 \pm 1.06 |
| AR2 | Proteobacteria | <i>Achromobacter insuavis</i> | 96.47 \pm 0.10 | 15.45 \pm 1.41 | - | 19.6 \pm 0.71 |
| 19VE21-2 | Proteobacteria | <i>Achromobacter xylosoxidans</i> | 94.05\pm0.10 | 78.64\pm0.50 | 31.91\pm0.53 | 85\pm0.71 |
| 19VE21-3 | Proteobacteria | <i>Achromobacter xylosoxidans</i> | 94.64\pm0.10 | 76.82\pm0.10 | 28.82\pm3.50 | 86.3\pm2.25 |
| P.Fluc | Proteobacteria | <i>Pseudomonas fluorescens</i> | 95.23\pm0.71 | 87.08\pm0.10 | - | 62.1\pm3.18 |

2.2. In vitro antagonism screening against grape fungal pathogens and volatile effect

The ability of bacterial isolates to control *Botrytis cinerea* (the bunch grey mold causal agent), *Phaeoacremonium minimum*, *Neofusicoccum parvum* (the latter two are key players in the wood esca syndrome) and *Guignardia bidwellii* (the black rot causal agent) was evaluated *in vitro*. To perform biocontrol activity tests, each isolate was grown on solid media (CYA) for at least 5 days and then inoculated four times at the edge of a 90 mm Petri dish containing CYA media. The specific pathogen was inoculated 48 hours later as a mycelial plug or conidial suspension according to the specific pathogen characteristics and then monitored for growth. Each combination of bacterial isolate and fungal pathogen was made in triplicate and the colony diameter measured twice for each biological replicate and each time point. For *B. cinerea* and *N. parvum* (both considered as fast-growing fungi) the biocontrol assay lasted 10 days at 28 °C in dark conditions, for *P. minimum* and *G. bidwellii* (both considered slow-growing fungi) the assay lasted 20 days at 28 °C in dark conditions. Inhibition percentages were calculated measuring the colony diameters on CYA of pathogens alone or in the presence of bacterial isolates. The growth ratio was obtained by dividing the colony diameter on CYA with the bacteria over the colony diameter on CYA alone.

Additionally, when inhibition was observed, the potential antifungal activity of volatile organic compounds (VOCs) was evaluated according to Oukala et al. (2021). In detail, the two room-plate method was used against the fungal pathogens reported above using at least three replicates for each bacterial isolate. After incubation at 28 °C, the percentage of mycelial growth inhibition was recorded and compared with their respective controls (Table 1).

The seven best performing isolates showing biocontrol activities against at least three pathogens, with at least one of them exhibiting a growth inhibition rate greater than 45%, were selected for the evaluation of potential PGP traits (see below) and for consortium formulation (Table 1; Figure S1), adopting the so-called bottom-up approach for the development of the SynCom (Sandrini et al., 2022a).

2.3. In vitro evaluation of plant growth promoting traits and compatibility test

In vitro compatibility test was performed in triplicate among the seven selected isolates (Table 1, bold highlighted isolates) on CYA plates. Each bacterial strain, after overnight culture (500 μ L, CYA media), was streaked onto solid media plates and co-cultured with each of the others. After ten days of incubation at 28 °C, the bacterial growth

was compared with a control plate where the isolate was cultured alone and, if present, inhibition effects were reported.

The selected isolates were also screened and evaluated for different PGP traits as previously described: production of indole acetic acid (IAA) (Guerrieri et al., 2020), ACC-deaminase activity (Li et al., 2011), siderophore production (Louden et al., 2011), N fixation (Geetha et al., 2014) using Jensen's Nitrogen Free bacteria (JNFB) medium, phosphorus solubilization (Singh et al., 2020), starch hydrolyzation (Kokare et al., 2004) and salt stress resilience at diverse % of NaCl (0%, 1.5%, 3% w/v) (Gopalakrishnan et al., 2014) using qualitative or quantitative methods (Table S1).

2.4. Plant inoculation and field experiments

Two hundred and thirty cuttings of the 'Pinot gris' cultivar, grafted onto Kober 5BB rootstock and certified as 'virus free', were purchased from an Italian nursery (Vivai Cooperativi Rauscedo, Italy; <http://www.vivairauscedo.com>). Cuttings were treated as previously reported in (Nerva et al., 2022b) prior to plantation. Three treatments were compared in this study: i) non-treated control plants, CTRL; ii) 7-bacterial consortium-inoculated plants, SynCom; iii) SynCom-inoculated plants with a commercial consortium formed by different AMF species and the rhizosphere bacterial strain *Bacillus coagulans*, AMF+B. The experiments were repeated twice during the season, two independent rounds of cuttings inoculation and transplanting were thus performed for both SynComs (50+50 plants for each), while 15 and 15 uninoculated plants were used as CTRLs for the first and second round of experiments.

As cited before, in this study we developed a 7-bacterial consortium with isolates showing antagonistic activities previously isolated from grapevine woody tissues (see above) (Nerva et al., 2022a). The seven selected and compatible bacterial strains were grown in liquid CYA medium for 48 hours, then bacteria were collected using a centrifuge and resuspended in sterile water. Bacteria were counted and diluted to 10^9 cells mL⁻¹. The single bacterial suspensions were mixed to form the SynCom and inoculated into roots of one-year-old 'Pinot gris' cuttings using an equal volume of each strain ($\sim 10^8$ cells mL⁻¹). In detail, prior to field planting, cuttings were maintained for 30 days in a plastic container filled with sterilized substrate (80% sand and 20% peat) supplemented with the formulated SynCom to a final concentration of 10^6 cells mL⁻¹ of substrate. For the AMF+B treatment, the grapevine cuttings were inoculated with a commercial soluble powder-based SynCom (MycoApply® DR formulation, Sumitomo Chemical Agro Europe SAS), formed by an AMF mixed inoculum (*Rhizopagus irregularis*, *Claroideoglossum luteum*, *Claroideoglossum etunicatum*, *Claroideoglossum claroideum* corresponding to 1% of the total inoculum as reported on the label) and by a rhizospheric bacterium (*Bacillus coagulans*, 2'180'000 UFC g⁻¹), following the manufacturer's instruction (the inoculum was resuspended in sterile water to use the same conditions as the formulated consortium). As for the 7-strain consortium, AMF+B-inoculated cuttings were maintained for 30 days in containers with steam sterilized substrate amended with the commercial inoculum. For CTRL plants, cuttings were prepared similarly and maintained on the same substrate for 30 days but without any microbial inoculum.

Trials were conducted in a semi-controlled experimental field, specifically dedicated to this experiment, located at Cantine Rauscedo, Rauscedo, Italy (GPS coordinates: 46.054978N, 12.816345E). The field was trained as a commercial vineyard with regular pruning to shape the vine's canopy according to the chosen training system, thus standardizing the plant's growth and creating appropriate microclimatic conditions. For this reason, it was not possible to measure the growth parameters over the season. The about 3000 m² of vineyard available for this study was composed of a sandy loam soil (pH 7.3; available P 8.4 mg kg⁻¹; organic matter 1.70%; cation exchange capacity 22.11 mew 100 g⁻¹) that had not been cultivated for three consecutive years prior to our experiments. After 60 days from field planting, leaf ecophysiological

measurements and sampling of leaf and root tissues for molecular and biochemical analyses were performed. The collected samples were freeze-dried and stored at -80 °C until use. A part of the root apparatus was used to estimate the level of mycorrhizal colonization [i.e., arbuscule abundance in the root system by morphological observation of thin roots fragments as previously described (Chitarra et al., 2016; Nerva et al., 2021)]. Fungal colonization was then quantified according to the Trouvelot system (Trouvelot et al., 1986) and using the MYCOCALC software. The following parameters were considered: F% frequency of mycorrhiza in the root system, M% intensity of mycorrhizal colonization in the root system, a% arbuscule abundance in mycorrhizal parts of root fragments, A% arbuscule abundance in the root system, v% vesicle abundance in mycorrhizal parts of root fragments. Data obtained from the two independent experiments were collected and biological replicates were mediated and analyzed. The impact of the inoculated bacterial consortium on rhizosphere microbial community structures and their indirect colonization efficiency was evaluated as previously reported by Kaur et al. (2022). This was performed through amplicon sequencing analysis of root samples (see below).

2.5. Leaf gas exchange measurements

Instantaneous measurements of net photosynthesis (Pn), stomatal conductance (g_s), intercellular CO₂ concentration (Ci), apparent carboxylation efficiency (ACE, calculated as the ratio between Pn and Ci) and intrinsic water use efficiency (iWUE, defined as the ratio between Pn and g_s) were carried out on six randomly selected vines from each treatment for the two independent experiments. For each plant, three fully developed non-senescent leaves of the same physiological age (4th to 5th leaf from the shoot apex, n=36 per treatment) were measured, using a portable infrared gas analyzer (ADC-LCi T system; Analytical Development Company, BioScientific Ltd., UK), as previously reported (Belfiore et al., 2021). The measurements were taken using ambient parameters, as follows: light intensity ranged from 1.600 to 1.700 μmol photons m⁻² s⁻¹, ambient temperature ranged from 25 to 28 °C, and CO₂ concentration in the air ranged from 420 to 440 ppm.

2.6. Targeted metabolite analysis

Freeze-dried leaf and root collected samples were used to determine *t*-resveratrol and viniferin concentrations using a high-performance liquid chromatographer (HPLC), as previously reported (Nerva et al., 2022a; Nerva et al., 2022b). In parallel, roots were collected from the same plants, immediately frozen in liquid nitrogen, freeze-dried and stored at -80 °C until use.

To analyze changes in the accumulation of defense-related hormones (methyl salicylate, methyl jasmonate and jasmonic acid), the same lyophilized root and leaf samples were extracted as previously described (Huang et al., 2015). The extracts were injected into an Agilent 6890N-5973i mass spectrometer. Chromatographic separation was performed using a Restek Rxi-5ms column (30 m × 0.25 mm × 0.25 μm) to ensure high-resolution and reliable quantification of the analytes (Restek Corporation, Bellefonte, PA, USA). The injection parameters were set at a temperature of 280 °C and volume of 2 μL, with a helium flow rate of 1.1 mL min⁻¹. The Selected-Ion Monitoring (SIM) mode was utilized to enhance both the accuracy and sensitivity of the method. In contrast to Huang et al. (2015), specific ions were employed for the quantification of each analyte. For instance, salicylic acid was quantified at an m/z of 138 and identified through m/z values of 92 and 120. Methyl salicylate was quantified using m/z 152 and identified at m/z values of 120 and 92. Jasmonic acid was quantified at an m/z of 210 and identified at m/z values of 151 and 83. Lastly, methyl jasmonate was quantified using m/z 224 and identified through m/z values of 151 and 83. Electron ionization was conducted at 70 eV, with source and quadrupole temperatures optimized at 230 °C and 150 °C, respectively.

2.7. RNA isolation, cDNA synthesis, qPCR analysis and RNA sequencing

The same root and leaf samples collected for metabolite analysis were processed to isolate RNA starting from at least 50 mg of lyophilized tissue, using the Spectrum™ Plant Total RNA Kit (Sigma-Aldrich), following the manufacturer's instructions. RNA concentrations were checked with a Nanodrop™ (Thermo Fisher Scientific) apparatus. RNA samples were then treated with DNase I (Thermo Fisher Scientific), according to the manufacturer's instructions. The absence of DNA contamination was further checked prior to cDNA synthesis by quantitative real-time PCR (qPCR) using *VvCOX* (cytochrome oxidase) grapevine specific primer (Table S2). After DNase treatment, samples were subjected to cDNA synthesis using the High-Capacity cDNA Reverse Transcription Kit (Applied Biosystems, Thermo Fisher Scientific), starting from 500 µg of total RNA. qPCR runs were performed in a final volume of 10 µL using the SYBR® green chemistry (Bio-Rad Laboratories Inc.) and 1:5 diluted cDNA as template. Reactions were conducted in a Bio-Rad CFX96 instrument (Bio-Rad Laboratories Inc.) as previously described (Nerva et al., 2022c). Transcript relative expression levels were calculated according to the comparative cycle threshold (CT) method (Livak and Schmittgen, 2001) using two reference genes (*VvCOX* and ubiquitin, *VvUBI*) for gene expression normalization. Oligonucleotide sequences are listed in Table S2. Gene expression data were calculated as expression ratio (relative quantity, RQ) to CTRL plants. For each analyzed gene, melting curve data are reported in Table S3.

To gain information on the systemic molecular signature triggered by the inoculated SynCom consortium, RNA isolated from SynCom and CTRL leaf samples was submitted to library preparation and sequencing. To proceed with RNAseq analysis, an average of four µg per sample were sent to Macrogen Inc. (South Korea), where cDNA libraries were built (TrueSeq total RNA sample kit, Illumina) and sequenced adopting the Illumina Novaseq technology, with an average output of 40M paired end reads (100 bp length) for each sample.

The Artificial Intelligence RNA-seq Software AIR (accessible at <https://transcriptomics.cloud>) was used to analyze RNA-seq data. AIR accepts as input file the raw next generation sequencing Illumina data (fastq format). RNA-seq data were uploaded to the cloud and validated to automatically pair forward and reverse files, as well as check their format and integrity. Quality analysis was assessed using FastQC. The forward analysis included quality trimming and Differential Gene Expression (DGE) followed by a Gene Ontology Enrichment Analysis (GOEA) using the V1 version of the grape PN40024 transcriptome (Minio and Cantu, 2022). Once the analysis was launched, bad quality reads were removed using BBDuk by setting a minimum length of 35 bp and a minimum Phred-quality score of 25. Afterwards, high quality reads were mapped against the reference genome using STAR (Dobin et al., 2013) with the end-to-end alignment mode, and gene expression quantification was performed with featureCounts (Liao et al., 2014). Transcripts were annotated using the V1 version of the reference grapevine genome and grouped into functional gene classes according to VitisNet GO (Grimplet et al., 2012). Heat maps of transcriptional profiles associated with specific functional categories were generated with TMeV 4.9 (<http://www.tm4.org/mev.html>), using the average expression value (FPKM) of the three biological replicates as input. The BiNGO 3.0 plug-in tool in Cytoscape (v3.2, U.S. National Institute of General Medical Sciences (NIGMS), Bethesda, MD, USA) was used for running the GO enrichment analysis (Maere et al., 21). Over-represented Plant GO slim categories were then identified using a hypergeometric test setting the significance threshold at 0.05. Differentially expressed genes (DEGs) were identified in a pairwise comparison (SynCom vs CTRL) using a p-value of 0.05% adjusted with the Benjamin-Hochberg method and setting the fold change threshold (\log_2 transformed FPKM values of the SynCom/CTRL ratio) at $\geq +1$ or ≤ -1 .

2.8. Root DNA isolation and metabarcoding analysis

Starting from the root samples used for RNA isolation, about 50 mg were used to extract DNA following the manufacturer's instructions of the plant/fungi DNA isolation kit (Norgen Biotech Corp., Thorold, ON, Canada), as previously reported (Nerva et al., 2021). For each treatment, four biological replicates were extracted by randomly selecting plants from the two experimental replications. Total DNA was quantified using a NanoDrop One spectrophotometer (Thermo Fisher Scientific, Waltham, MA, USA), and DNA integrity was inspected running the extracted samples on a 1% agarose electrophoretic gel. While preparing the samples for sequencing, a further quantification was performed using a Qubit 4 Fluorometer (Thermo Fisher Scientific, Waltham, MA, USA) to compare and integrate the previous quantifications.

To analyze the root-associated bacterial community the V3-V4 hypervariable region of the 16S rRNA gene was targeted by the universal primers 319F (5'-CCTACGGGNGGCWGCAG-3') and 806R (5'-GAC-TACHVGGGTATCTAATCC-3'). For the inspection of the root-associated fungal community the ITS2 region of the rRNA gene was analyzed using the primers ITS3 (5'-GCATCGATGAAGAAGCAGC-3') and ITS4 (5'-TCCTCCGTTATTGATATGC-3'). The *ad hoc* designed peptide nucleotide acid (PNA) blocker oligos (Kaneka Eurogentec S.A., Belgium) for *V. vinifera* were used to inhibit plant material amplification allowing plant DNA contamination < 5% (Lundberg et al., 2013; Cregger et al., 2018; Nerva et al., 2021). A first strict quality control on raw data was performed with FLASH (Magoč and Salzberg, 2011) and then processed with two independent Qiime2 (Bolyen et al., 2019) pipelines. To analyze the bacterial community, the 16S rRNA gene sequences were subjected to quality filtering with DADA2 (Callahan et al., 2016). Feature sequences were summarized and annotated using the RDP classifier (Cole et al., 2014) trained to the full length 16S database retrieved from the curated SILVA database (v138) (Quast et al., 2012). For graphic representation, only genera with an average relative abundance higher than the settled threshold (2%) were retained, with the exception of genera recalling the inoculated isolates.

To analyze the fungal community through ITS2 rRNA genomic sequences, reads were first filtered using the hidden Markov models (HMM) (Rivers et al., 2018). Briefly, the software allows true sequences to be distinguished from sequencing errors, filtering out reads with errors or reads without ITS sequences. To distinguish true sequences from those containing errors, sequences were sorted by abundance and then clustered in a greedy fashion at a threshold percentage of identity (97%). Trimmed sequences were analyzed with DADA2 and sequence variants were taxonomically classified through the UNITE database (Abarenkov et al., 2010). For graphic representation, only genera with an average relative abundance higher than the settled threshold (1%) were retained with the exception of genera of inoculated mycorrhizal fungi. Co-occurrence Network interference (CoNet v1.1.1.beta) (Faust and Raes, 2012, 2016) was employed to identify significant co-occurrence patterns among the microbial communities, as previously reported (Nerva et al., 2021).

2.9. Statistics

Ecophysiological, biochemical, qPCR gene expression and AMF colonization data were analyzed by the one-way analysis of variance (ANOVA). When ANOVA was significant, mean separation was performed according to Tukey's *HSD* test at a probability level of $P \leq 0.05$. Standard deviation (SD) or error (SE) of all means was calculated. The SPSS statistical software package (version 22) was used to run statistical analyses.

Microbial data were analyzed using the qiime2-implemented functions (Kruskal-Wallis test, Permanova). Ecological indices (*i.e.*, NMDS and PERMANOVA) were calculated in Past4.04. RNAseq data were analyzed using dedicated pipelines in Artificial Intelligence RNA-seq Software AIR (accessible at <https://transcriptomics.cloud>).

3. Results

3.1. Isolation and molecular characterization of the bacterial collection

Forty-four bacterial isolates were collected, and the molecular identification was achieved by 16S rRNA gene sequencing analysis. The molecular identification showed that several of them belonged to the Actinobacteria phylum (Table 1). However, although a specific protocol for Actinobacteria isolation was adopted, only 22 out of the 44 isolates were Actinobacteria, while the remaining 22 were Proteobacteria (Table 1). Checking in the literature, none of the bacterial isolates showed similarities with those harmful for humans or plants. The 16S sequences of each isolate were deposited in NCBI GenBank under the accessions OP994307-OP994344.

3.2. In vitro evaluation of biocontrol and Plant Growth Promoting (PGP) activities of the bacterial isolates

To further characterize these isolates, all 44 bacterial strains were *in vitro* assessed for biocontrol activity against some of the most important and widespread grapevine pathogens (Table 1). In the biocontrol Petri dish assay, the considered strains showed a different degree of pathogen containment and the best performing isolates, considering all pathogens and the ability to grow together, were selected as good candidates to build a SynCom (Table 1 and Figure S1). Particularly, an antagonistic activity towards at least three pathogens and a pathogen growth inhibition rate higher than 45%, facing at least one fungus, was adopted as selection criterion. The seven selected bacterial strains are highlighted in bold in Table 1. Further analyses were performed to evaluate the ability of SynCom candidate members to stimulate plant growth and abiotic stress tolerance (Table S1): all seven candidates were able to solubilize starch, with the 19VE21-2 isolate showing the largest halo zone around the colonies. Four isolates out of the seven were able to solubilize phosphate, with 19VE21-2 showing the widest clear zone around the colonies. Three isolates were able to grow on Nfb agar plate thus showing a potential to fix nitrogen, and among those, ACT2 showed the most preeminent growth. Five isolates were proved to be siderophore producers, with ACT25 and 19VE21-3 showing the widest yellow halo appearance around bacterial colonies on the Chrome Azurol medium. Five isolates were identified as IAA producers, and P. Fluo was the one showing the most abundant IAA production. Four strains were also able to degrade ACC, and particularly the ACT35 and 19VE21-2 isolates displayed the highest consumption activities. As the last PGP-related trait, we evaluated the ability of the selected isolates to grow in the presence of NaCl at different concentrations (0, 1.5 and 3% w/v), and we found that six out of the seven candidates displayed an enhanced salinity tolerance. The biocontrol activity and PGP-traits are reported in Fig. 1 for each of the selected isolates, along with pictures taken at the end of the biocontrol assay on *Guignardia bidwellii* (the causal agent of black rot). Finally, to limit reciprocal inhibition effects, a strain compatibility assay was performed. The results revealed a good aptitude of the candidates to live together without inhibition haloes, thereby confirming them as promising members to form a grape-specific consortium (see the example reported in Fig. S2).

3.3. Analysis of AM colonization in the root

To confirm the establishment of mycorrhizal symbiosis in roots of plants inoculated with the commercial mixed formulation (AMF+B), colonization in root cortical cells was evaluated on three randomly selected plants for each treatment. Microscopic observations of stained roots revealed the presence of mycorrhizal structures to different extent depending on the treatment. The roots of AMF+B treated plants had a significantly higher percentage of mycorrhization frequency (F), ranging around 100%; intensity of the mycorrhizal colonization in either the root system (M) or fragments (m) ranged around 60%; the arbuscule

abundance ranged around 94% in root fragments (a) and around 54% in the root system (A) (Fig. S3a). Conversely, very few fungal structures were observed in the roots collected from SynCom and CTRL samples (Fig. S3a). Additionally, to check the functionality of AM symbiosis, 3 AM symbiosis-related genes (*i.e.*, *VvCCD7* and *VvCCD8*, both involved in strigolactone biosynthesis, and *VvPTI-3*, encoding a putative grape phosphate transporter) were analyzed. Expression of *VvCCD7* was significantly up-regulated in AMF+B- and SynCom-treated plants with respect to CTRL plants (Fig. S3b), while expression of *VvCCD8* did not vary significantly among treatments (Fig. S3c). The *VvPTI-3* gene was previously reported as a marker of functional AM symbiosis establishment (Balestrini et al., 2017; Nerva et al., 2022b). Here, its expression significantly increased in AMF+B samples with respect to CTRL and SynCom samples (Fig. S3d). Overall, these results demonstrated that AMF+B roots were efficiently colonized, and that AM symbiosis was successfully established in the grapevine cuttings. Conversely, colonization from native AMF in SynCom and CTRL plants was not relevant.

3.4. Microbiome analysis of root-associated endophytes and pathogens

To understand the effects of SynCom and AMF+B on root-associated microbial communities, including the naturally occurring wood decay pathogens, samples were processed for bacterial and fungal profiling (detailed results of sequencing are reported in Table S4). Shannon index diversity indicated that AMF+B-treated samples had a significantly higher bacterial diversity in comparison to both CTRL and SynCom, while SynCom did not differ from CTRL (Table S5). Shannon index for the fungal community attested that all treatments significantly differed from each other. Specifically, AMF+B samples exhibited the highest diversity, followed by CTRL, and SynCom (Table S5). The non-metric multidimensional scaling (NMDS), based on Bray-Curtis dissimilarity matrixes, highlighted that both bacterial (Fig. S4a) and fungal communities (Fig. S4b) were significantly influenced by the treatment applied. These results were also confirmed by PERMANOVA analysis, from which a significant distinction emerged between bacterial and fungal communities in all tested conditions (Fig. S4).

The composition of the bacteria community at genus level is reported for each sample type in Supplementary Table S6. A graphic distribution of the taxa representing at least 1% of the community is displayed in Fig. 1a. The comparison of the bacterial community among treatments revealed that the genus *Pelosinus* (phylum Firmicutes) was negatively affected by the inoculation of both AMF+B and SynCom. On the contrary, abundance of the genus *Flavobacterium* (phylum Gammaproteobacteria) was positively modulated by both AMF+B and SynCom treatments. In parallel, amplicon sequence variant (ASV) belonging to the genera inoculated with the SynCom (*i.e.*, *Pseudomonas*, *Asanoa*, *Achromobacter*, *Actinomadura*, *Rhizobium* and *Methylobacteria*) was significantly overrepresented in the SynCom samples (Supplementary Table S6).

The fungal community composition at genus level is reported in Supplementary Table S7 for each sample type. A graphic outline of the taxa representing at least 1% of the community is shown in Fig. 1b. A further comparison of the fungal community among treatments revealed interesting outputs. The *Claroideoglossum* genus, belonging to the Glomeromycota phylum, was overrepresented only in the AMF+B samples where mycorrhizal fungi were added. In parallel, the *Neofusicoccum*, *Phaeoconiella* and *Phaeoacremonium* genera, commonly associated with wood decay, were underrepresented in the SynCom-treated plants with respect to AMF+B and CTRL plants (Supplementary Table S7).

The network analysis of microbial communities, performed among the different treatments and conducted using the co-occurrence method, is detailed in Supplementary Table S8 and depicted in Fig. S5. Co-occurrence networks were calculated by combining data from 16S and ITS sequencing analyses for CTRL (Fig. S5a), AMF+B (Fig. S5b) and SynCom (Fig. S5c). Additionally, root biochemical measurements were incorporated as features during the analysis process.

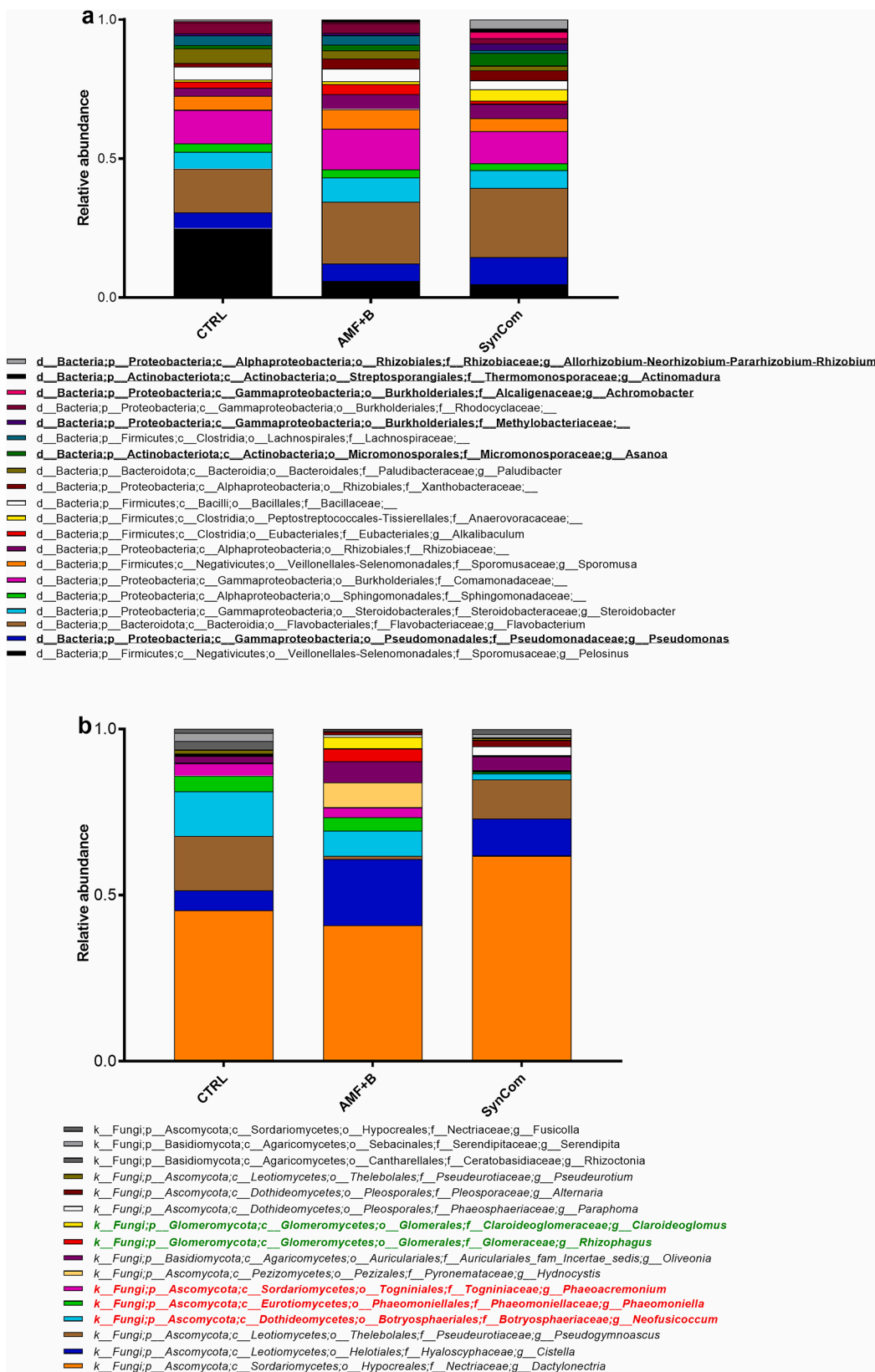


Fig. 1. Relative abundances of bacterial and fungal genera. a) Bacterial genera added with SynCom inoculation are highlighted in bold. Only genera representing at least 1% over the total classified amplicons were retained. b) Fungal genera belonging to mycorrhizal species added with the commercial formulation (AMF+B) are highlighted in green. Wood decay-associated fungal genera are highlighted in red. Only genera representing at least 1% over the total classified amplicons were retained.

Interestingly, when the whole dataset was analyzed, the co-occurrence network highlighted a significant mutual exclusion effect between some of the bacteria inoculated with the SynCom consortium and wood fungal pathogens (Supplementary Table S8 – sheet d). Among these interactions, the *Asanoa* genus displayed a mutual exclusion correlation with all the wood fungal pathogens previously considered (i.e., genera *Neofusicoccum*, *Phaeoconiella* and *Phaeoacremonium*). On the contrary, the fungal pathogens were all linked by a copresence correlation.

3.5. Outline of physiological and biochemical responses in field conditions

The leaf gas exchange rates were measured in treated vines to establish whether inoculation with SynCom could modify the plant physiological performances in open field conditions. Rooted cuttings previously inoculated with AMF+B had a significantly higher Net Photosynthesis (Pn) when compared to CTRL and SynCom-treated plants, whereas the latter showed the significantly lowest Pn values when compared both to AMF+B and CTRL treatments (Fig. 2a). The rates of stomatal conductance (g_s) significantly increased following the AMF+B treatment with respect to the other conditions. No significant

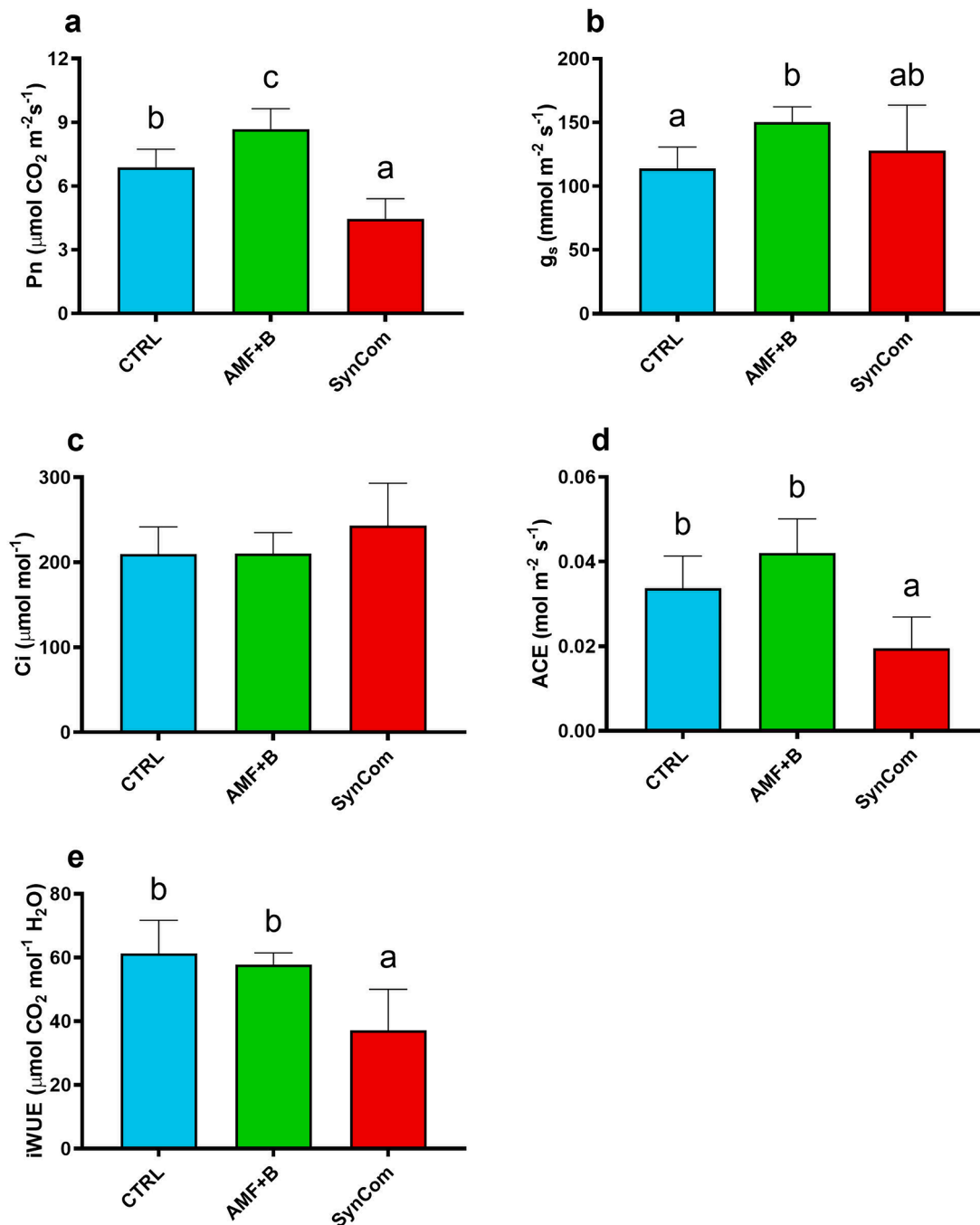


Fig. 2. Instantaneous leaf gas exchange measurements. Values of a) net photosynthesis (Pn); b) stomatal conductance (g_s); c) intercellular CO_2 concentration (Ci); d) apparent carboxylation efficiency (ACE); and e) intrinsic water use efficiency (iWUE) recorded in CTRL (control), AMF+B, (commercial AMF + Bacteria mixed inoculum)-treated and SynCom (Synthetic Community)-treated plants. Data are expressed as mean \pm SD ($n = 36$). Different lowercase letters above bars indicate significant differences according to Tukey's HSD test ($P < 0.05$).

rise in g_s was also observed in SynCom-treated vines in comparison with CTRL (Fig. 2b). Conversely, the values of substomatal CO_2 concentration (Ci) did not significantly change in the analyzed plants, independently of treatment (Fig. 2c). Additionally, the Apparent Carboxylation Efficiency (ACE) and the intrinsic Water Use Efficiency (iWUE) were calculated, highlighting significantly lower values in the SynCom-treated plants with respect to all other conditions (Fig. 2d,e). Overall, the analysis of ecophysiological parameters pointed to a photosynthetic imbalance in the SynCom-inoculated vines.

Changes in grapevine metabolism occurring in both leaves and roots were inspected by analyzing the accumulation of secondary metabolites involved in defence processes (i.e., *t*-resveratrol, viniferin). The concentration of defensive secondary metabolites was overall more accentuated in both leaves and roots of inoculated plants. In detail, leaf samples collected from the SynCom-treated plants showed the highest *t*-resveratrol concentrations, up to three-fold those measured in CTRL leaves (Fig. 3a). Compared with CTRL, *t*-resveratrol production was strongly elicited in the roots of inoculated plants, with similar values between SynCom and AMF+B-treated plants (Fig. 3b). Viniferin amounts were almost undetectable in the leaf of not treated vines, but significantly increased following SynCom and AMF+B inoculation (Fig. 3c). Similar accumulation patterns were observed for viniferin quantification in root tissues (Fig. 3d).

Along with stilbenoids, changes in the content of other core components of the ISR/SAR immune system were investigated. Methyl jasmonate (MJ), and jasmonate (JA) were quantified in the target tissues in addition to methyl salicylate (MS), a key component of SAR (Fig. S6). The obtained data indicated that MS and JA levels were not influenced by the treatments adopted. The concentrations of these compounds did not in fact significantly differ among the tested conditions in either root

or leaf tissues (Fig. S6a-b). Although MJ levels in the leaf did not vary among the diverse treatments (Fig. S6a), a significant increase was observed in the root of SynCom-inoculated vines with respect to CTRL plants (Fig. S6b).

3.6. Expression profiles of key target genes involved in defence response and chlorophyll degradation

Regarding genes associated with the establishment of defence mechanisms, the expression of *VvPAL*, which encoded a phenylalanine ammonium lyase, was significantly higher (more than two-fold) in both leaves and roots of AMF+B- and SynCom-treated plants with respect to CTRL (Fig. 4a,b). Particularly, the leaves of SynCom-inoculated plants displayed the highest *VvPAL* expression rates. Conversely, in the roots, the transcriptional levels of the gene were similar between AMF+B and SynCom plants (Fig. 4a,b). A similar expression pattern was observed for *VvSTS1*, encoding a grapevine stilbene synthase, the transcription of which was significantly higher in the leaves of both AMF+B and SynCom plants, regardless of the specific treatment (Fig. 4c). Nonetheless, *VvSTS1* expression levels were lower in root samples collected from AMF+B- and SynCom-inoculated vines than CTRL, although the gene downregulation was statistically significant only in AMF+B roots (Fig. 4d). Looking at key players of the plant immunity system, both *VvLOX*, encoding a lipoxygenase, and *VvNPR1*, a non-expressor of pathogenesis-related genes 1, are well known genes involved in the onset of ISR (JA-mediated) and SAR (SA-mediated), respectively. Independently of the tissue, transcription of *VvLOX* was significantly up-regulated exclusively upon SynCom treatment, showing expression values up to 2-fold higher than AMF+B and CTRL samples (Fig. 4e-f). Although no significant differences among treatments were observed for

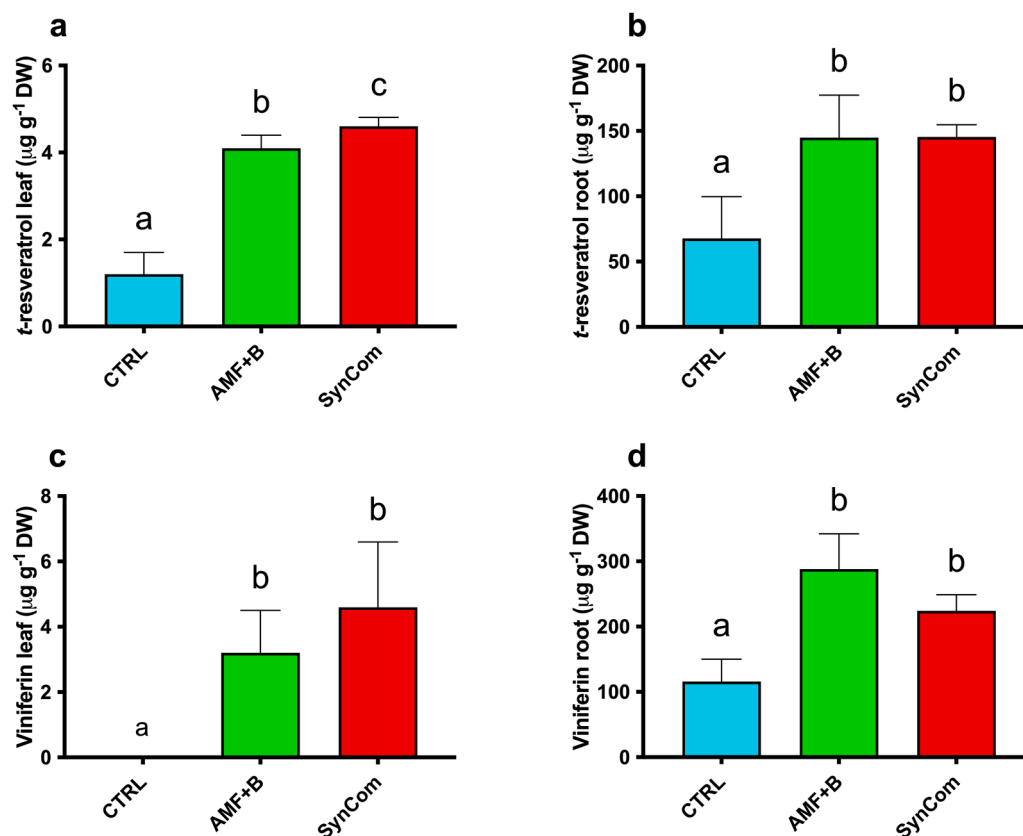


Fig. 3. Concentrations of target metabolites in leaf and root tissues. a,b) *trans*-resveratrol (*t*-resveratrol) quantification in leaf and root tissues, respectively. c,d) Viniferin quantification in leaf and root tissues, respectively. Data are expressed as mean \pm SD ($n = 3$). Different lowercase letters above bars indicate significant differences according to Tukey's HSD test ($P < 0.05$). CTRL, control plants; AMF+B, commercial AMF + Bacteria mixed inoculum-treated plants; SynCom, Synthetic Community-treated plants.

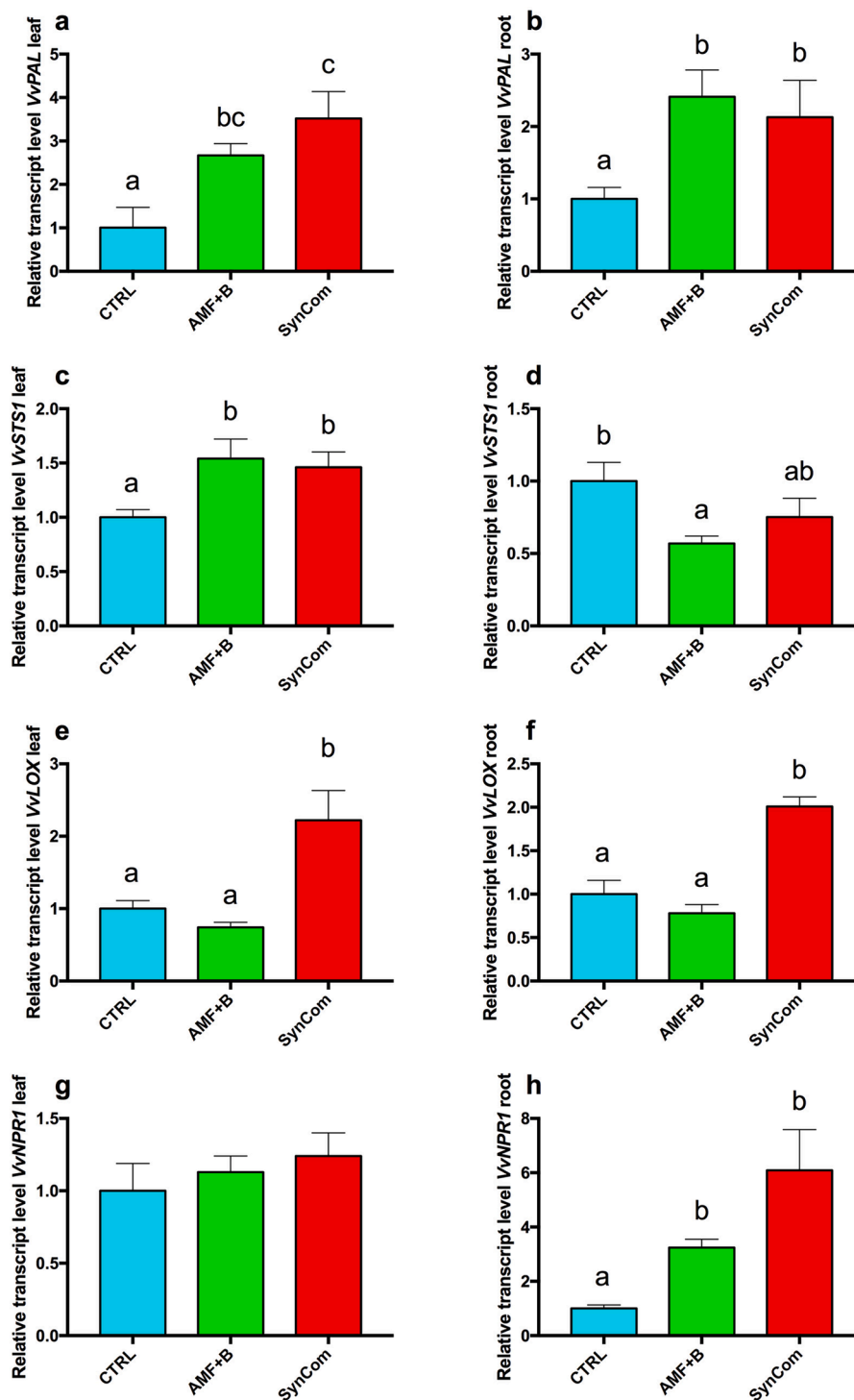


Fig. 4. Expression changes of defence-related genes. a,b) Relative expression level of *VvPAL* in leaf and root tissues, respectively. c,d) Relative expression level of *VvSTS1* in leaf and root tissues, respectively. e,f) Relative expression level of *VvLOX* in leaf and root tissues, respectively. g,h) Relative expression level of *VvNPR1* in leaf and root tissues, respectively. Data are expressed as mean \pm SD ($n = 3$). Different lowercase letters above bars indicate significant differences according to Tukey's HSD test ($P < 0.05$). CTRL, control plants; AMF+B, commercial AMF + Bacteria mixed inoculum-treated plants; SynCom, Synthetic Community-treated plants.

VvNPR1 expression in the leaves (Fig. 4g), transcription of this gene was significantly highly induced in the roots of AMF+B- and SynCom-treated plants, with expression values up to about 4- and 6-fold higher than CTRL plants, respectively (Fig. 4h).

Finally, to support the changes observed in photosynthetic rates, *VvCHL*, a chlorophyllase-encoding gene was analyzed. *VvCHL* showed significantly higher transcriptional values in the leaves of SynCom-

treated plants with respect to samples collected from AMF+B and CTRL vines (Fig. S7).

3.7. Focus on SynCom-mediated whole transcriptome reprogramming in the leaf

In search of further experimental evidence strengthening the

SynCom-mediated activation of systemic defence signaling routes, whole transcriptome changes were analyzed by high-throughput sequencing (RNAseq) in the leaves collected from SynCom-treated plants. RNAseq data were first processed to identify those transcripts that were differentially expressed in the SynCom vs CTRL comparison, by applying a *P*-value adjusted with Benjamin-Hochberg $\leq 0.5\%$ and setting a fold-change threshold (\log_2 transformed FPKM values of the SynCom/CTRL ratio) of ≤ -1 or $\geq +1$. The output of this analysis indicated that 147 out of the 29970 annotated grapevine genes (V1 annotation of the PN40024 reference genome) were significantly differentially expressed (DEGs) in the SynCom vs CTRL comparison. Among the obtained DEGs, 142 were significantly up-regulated in leaves of SynCom-treated plants (Table S9), whilst only 5 were down-regulated (Table S10). This finding suggested that, despite the SynCom inoculation was successful in determining changes in the plant's physiological performances (Fig. 2) and in the accumulation of specific defensive metabolites (Fig. 3 and S6), the overall leaf transcriptomic alterations induced by this treatment were poor. Nevertheless, it is worth noting that almost all DEGs were up-regulated in SynCom leaves (Fig. 5a, Table S9). A Gene Ontology (GO) enrichment analysis, performed considering all DEGs, revealed that transport, response to endogenous stimulus, photosynthesis and energy metabolism were the overrepresented functional gene categories (Fig. 5b). Particularly, within the transport functional group, several transcripts encoding aquaporins and metal ion transporters were induced. In the other enriched categories, such as response to stress and hormone metabolism and signaling, transcripts

encoding lipoxygenases (e.g., *VvLOX*), ethylene and auxin responsive factors, alpha expansins, monooxygenases (e.g., *YUC3*), and stress-related proteins (e.g., *VvPAL*) were also up-regulated (Table S11). Cellular processes, signaling and homeostasis and energy metabolism also belonged to the up-regulated functional categories, and included genes encoding enzymes or proteins involved in cell wall metabolism (e.g., cellulose synthase, arabinogalactan protein) and photosynthesis (e.g., Ribulose 1,5-bisphosphate carboxylase, ferredoxin and photosystem I and II-related proteins). Conversely, three out of the five genes found significantly down-regulated in the SynCom vs CTRL comparison were associated with hormone metabolism, and specifically with jasmonate-mediated signaling pathways (Table S11).

The analysis of RNAseq data hence attested that, although the leaf transcriptome was poorly perturbed by SynCom inoculation, a constitutive activation of cell signaling and defence-related gene categories occurred, likely supporting the systemic nature of specific defence responses in these plants.

4. Discussion

In this study, a customized bacterial SynCom consortium, formed by seven potential endophyte strains with a marked *in vitro* biocontrol activity against *Vitis vinifera* fungal pathogens, was tested. Similarly, Liu et al. (2022) developed a SynCom composed of eight wheat-associated bacteria that effectively promoted the growth of inoculated wheat plants and reduced the *Fusarium pseudograminearum* (Fp) load, thereby

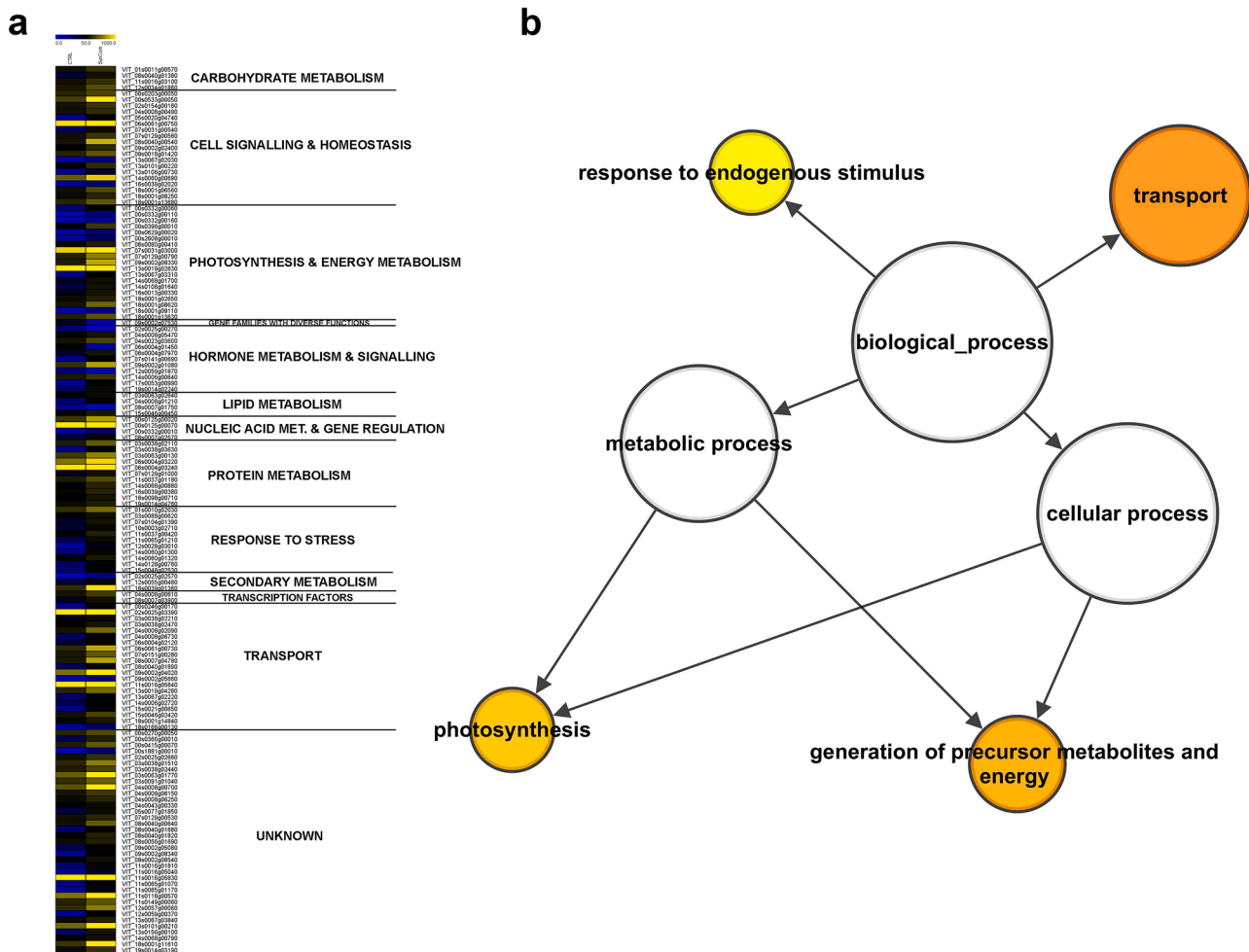


Fig. 5. Analysis of whole leaf transcriptome. a) MeV heat map of differentially expressed transcripts. Colour scale of the heat map chart ranges from blue (low expression) to yellow (high expression, FPKM > 50); **b)** Significant enriched GO biological functional categories obtained by applying Cytoscape with the BINGO plug-in on the whole DEGs dataset and listed according to their enrichment *p*-value ($P < 0.05$).

increasing plant survival rates. These authors suggested that using strains already adapted to the target plant environment could enhance inoculum survival, conferring more positive effects on plant growth and/or resistance traits. The number of isolates forming SynComs varied greatly among research studies, from 3–4 to hundreds, as previously reviewed in Sandrini et al. (2022a). Unlike herbaceous plant species, woody crops possess extended life cycles that hinder the characterization of the selected isolates *in planta*. This limitation prompted us to adopt a bottom-up approach, focusing on the selection of the most promising isolates based on *in vitro* evaluations (Sandrini et al., 2022a). In the present study, several isolates were proven to successfully limit the growth of different fungal pathogens, at least *in vitro*. Although the main objective was the development of a customized SynCom formed by biocontrol agents able to trigger direct and indirect defence responses, the seven isolated strains were also screened for some of the main PGP traits. Additionally, the identified bacteria were tested for tolerance to abiotic stress, *i.e.*, salt stress, which is a frequent issue in viticulture due to both high fertilization rates and the increasing incidence of drought events (Corwin, 2021). Among the seven PGP traits evaluated *in vitro*, each candidate isolate was found positive for at least two of the evaluated traits.

4.1. Field-grown plants inoculated with the customized SynCom showed impaired photosynthetic responses accompanied by a significant reduction of wood decay-associated pathogens

Only a few studies concern SynCom application in a glasshouse or experimental fields (Armanhi et al., 2021), and, to the best of our knowledge, none was conducted in grapevine, a recognized model woody crop (Nerva et al., 2022a). As already stated, our study was conceived to determine whether the application of synthetic communities (either customized or commercialized: SynCom or AMF+B, respectively) can represent a feasible approach in viticulture. The customized SynCom was inoculated on rooted cuttings before planting them, to foster the interaction establishment during the early developmental stages of rooted cuttings. Accordingly, Carlström et al. (2019) have recently demonstrated that community assembly is historically contingent and subject to priority effects, so that the early timing of microbiome inoculation is essential to obtain a stable SynCom in planta. Additionally, adult plants are characterized by rich and complex microbiomes that remain largely unaffected by latecomers (Toju et al., 2018). Individual strains of both Proteobacteria and Actinobacteria (both present in our SynCom) greatly affect the community structure as keystone species (Carlström et al., 2019). The metabarcoding data demonstrated that the species introduced with SynCom and AMF+B applications are significantly over-represented several months after inoculation (*i.e.*, at the end of the season). Although we could not track the inoculated fungi, it is feasible they derived from the initial treatment, as these fungal genera were only found in the AMF+B inoculated plants. The influence of plant-associated microorganisms on plant fitness has already been demonstrated (Yu et al., 2019). However, novel information on the effect of microbial inoculants on plant physiology is needed, and mainly when microorganisms are used in combination. Compared with CTRL, the two treatments differently modulated the vine's ecophysiology. Particularly, AMF+B-treated plants showed improved photosynthetic performances, suggesting that the synergic activity of AMF and rhizobacteria exerted a positive effect on plant fitness (Balestrini et al., 2020; Nerva et al., 2022b). Conversely, a negative impact on photosynthetic rates, ACE and iWUE was observed in SynCom-treated plants with respect to both AMF+B and CTRL ones. This finding was also consistent with changes in the expression profiles of *VvCHL*, a gene encoding a chlorophyllase (Chitarra et al., 2018), which was more transcribed in the leaves of SynCom-treated plants. These data suggested an overall photosynthetic imbalance in these plants, which occurred in parallel with a SynCom-based establishment of endogenous defence responses. Such a condition may therefore suggest a shift of

energy source allocation towards defence reaction signals.

Stilbenes, such as resveratrol and viniferin, are the main defence-related metabolites synthesized in grapevine and display well-documented antioxidant and antifungal properties, which are modulated by several factors, including the plant's associated microbiota (Verhagen et al., 2010). Moreover, beneficial microbes can trigger diverse ISR-related pathways, most of which are associated with the synthesis of stilbenes (Verhagen et al., 2010; Aziz et al., 2016; Nerva et al., 2022b). Both AMF+B and SynCom treatments led to a sharp increase in *t*-resveratrol and viniferin amounts in roots and leaves, highlighting a microbe-dependent synthesis of defensive compounds (Li et al., 2021; Nerva et al., 2022b). These findings also strengthened the notion that the primary mechanism for inducing systemic defense responses in grapevine involves the production and accumulation of stilbenes. Besides stilbenes, jasmonate is widely recognized as a key component of the ISR signaling in plants. Here, an enhanced biosynthesis of MJ was exclusively noticed in the roots of plants treated with AMF+B and SynCom, likely suggesting the establishment of localized rather than systemic defence responses in the treated plants.

Furthermore, to verify the impact of the two consortia application on the native microbial communities, a metabarcoding approach was adopted. Recent studies provide evidence that colonization by a SynCom in wheat, cotton and maize significantly impacts the plant physiological performances and also shifts native microbiomes and their interactions (Armanhi et al., 2018; Kaur et al., 2022; Liu et al., 2022). Metabarcoding analysis allowed the characterization of microbial populations associated with the roots three months after inoculation. Interestingly, AMF+B had a significant effect in reducing only abundance of the *Neofusicoccum* and *Phaeoacremonium* genera, whilst the impact of the SynCom treatment was stronger and evident also on the *Phaeomoniella* genus. In this context, it should be considered that grape wood pathogens are often associated with severe symptoms only when their abundance reaches a certain threshold (Nerva et al., 2022a). Furthermore, to understand whether the observed effects were due to either direct antagonistic or indirect plant-mediated interactions (Guo et al., 2021), the network co-occurrence of the microbial dataset was analyzed. The main AMF+B effects were addressed to the stimulation of resveratrol accumulation, which in turn was negatively correlated with pathogen relative abundance. Interestingly, the bacterial members of the SynCom displayed both a direct and indirect antagonistic effect. It is worth noting that the introduced species belonged to genera that were negatively correlated with wood pathogens, but which had a positive correlation with *t*-resveratrol and, more importantly, with viniferin, one of the most important antifungal molecules in grapevine, particularly effective also against the wood-related ones (Jeandet et al., 2002). Collectively, metabarcoding data indicated that the SynCom treatment could be more efficient than AMF+B inoculation in controlling wood fungal pathogens. This could likely be due to a combination of direct antagonistic interactions (*e.g.*, pathogen abundance was negatively correlated to the abundance of introduced bacterial species), as recently observed in SynCom-treated wheat plants infected by *Fp* (Liu et al., 2019).

4.2. Target responses controlling physiological and biochemical adjustments

Plants are known to finely tune their immune system during the interaction with beneficial microorganisms, regulating the expression of genes involved in different defence pathways (Alagna et al., 2020). Among the key defence-associated genes analyzed, *VvSTS1* (a stilbene synthase gene) was up-regulated in leaves of both SynCom and AMF+B plants and down-regulated in the roots of the same vines. Such an opposite trend could likely rely on the high amount of both resveratrol and viniferin in roots, which could play a negative regulation on the gene transcription. These data also confirmed a tissue-specific elicitation of the plant immunity responses (Nerva et al., 2022b). Notably, a role for stilbenes has been reported in controlling accommodation of beneficial

microorganisms in the roots and maintaining a homeostasis in the whole plant-associated microbial community (Liu et al., 2020).

At molecular level, the presence of treatment-dependent changes was also evaluated, looking at the expression of ISR- and SAR-related marker genes (*VvLOX* and *VvNPR1*, respectively), stress responsive and hormone-associated genes in root and leaf tissues.

Among defence-associated genes, the upregulation of *VvPAL* upon both treatments confirmed the elicitation of secondary metabolic pathways tied to defence (van Huylbroeck et al., 1998; Oh et al., 2009; Giudice et al., 2022), consistently with the significant increase in the stilbenes content in the same samples.

4.3. Leaf transcriptome profiling reveals the systemic nature of defence molecular signature in SynCom-treated plants

The findings discussed so far thus suggested that, following SynCom application, the endogenous plant's defence machinery was promptly turned on, even in the absence of external pathogen pressure. Such a condition resulted in the activation of specific molecular (e.g., exclusive *VvLOX* upregulation) and biochemical signals (e.g., higher amounts of MJ), and in peculiar physiological adjustments that were either absent or moderately induced upon AMF+B treatment. These achievements allowed us to hypothesize that SynCom-promoted defence signaling routes operated systemically. To provide evidence on this scenario, whole transcriptome reprogramming events were investigated in the leaf of SynCom-inoculated plants.

From a first analysis of sequencing data, it emerged that the leaf transcriptome was only poorly perturbed by the SynCom treatment. Only 147 genes were in fact found differentially expressed in comparison with the transcriptome of CTRL leaves, in agreement with previous studies conducted *in vitro* or in a controlled environment. Brotman et al. (2012) showed that *Arabidopsis* plants inoculated with a beneficial fungus at root level had improved resistance to the leaf pathogen *Pseudomonas syringae*. The authors proved that a systemic activation of the plant defence system already occurred in the inoculated plants before pathogen infection but without leading to a massive alteration of gene expression changes in the leaf (Brotman et al., 2012). Furthermore, following root colonization with the non-pathogenic bacteria *Pseudomonas fluorescens*, the onset of ISR signaling pathways observed in *Arabidopsis* leaves was not underlaid by an extensive transcriptome reprogramming (Verhagen et al., 2004).

Additionally, in our study, grouping of differentially expressed transcripts into functional categories highlighted an enrichment in gene clusters specifically involved in defence metabolic pathways and regulation of stress response. This data, associated with the fact that almost all DEGs were activated (142 out of 147 being upregulated), may further imply that the grapevine's interaction with the customized SynCom channeled the plant metabolism towards the activation of defence mechanisms, hence slowing down photosynthetic processes. Accordingly, a recent study reported a reduction in plant biomass and root growth and an overall low number of DEGs in the leaves of tomato plants inoculated with a microbial consortium (Prigigallo et al., 2023), in agreement with our results.

Our findings further proved that the SynCom-mediated trigger of defence metabolic pathways was not restricted to the root, and that a systemic activation of such responses was established resulting in a molecular signature at the leaf level.

5. Conclusion

In summary, a simplified SynCom formed by seven grape bacterial isolates was formulated and inoculated in young grape cuttings, following the priority effect principle. In addition to a non-inoculated control, the impact of the tailored SynCom was compared with that of a commercial inoculum (formed by diverse AMF and one rhizosphere bacterial species). The integration of physiological, biochemical and

molecular results provides a clear picture of the responses occurring between the plant and its inhabiting microbiome in field conditions (Fig. 6). Results showed that, at least under the considered experimental setup, the customized SynCom, formed by antagonistic bacteria with strong antibiosis activities against some fungal pathogens (i.e., wood-associated ones), successfully boosted the vine's defence machinery, leading to a significant reduction of wood-associated pathogens, while lowering photosynthetic performances.

Overall, our results provide new insights into grapevine responses following the application of a specifically formulated SynCom in comparison with a different formulated inoculum, containing both bacterial and AMF species not isolated from the target plants used in this study. On a broader perspective, our achievements demonstrated that the use of a targeted SynCom, formed by biocontrol agents directly isolated from grape plants, could be instrumental in nursery but also in those cultivated areas with high disease pressure, thus balancing the observed photosynthetic-defence trade-offs effects by ameliorating viticulture management practices in a sustainable way. Conversely, the results obtained using the AMF+B inoculum suggest that the trigger of defence responses could be potentiated, leading to improved eco-physiological performances and defence responses against pathogens in both aerial and underground parts of the plant although with less extent. These findings also imply that a cross-kingdom SynCom formulation based on bacterial endophytes and AMF can be implemented in future studies.

To date, most studies have adopted a similar reductionist model to assess the impact of SynCom on the host microbiome. The SynCom approach, however, is constrained to culturable bacteria, and the compatibility among microbial members remains a significant bottleneck for its application. Nonetheless, with the establishment of species-specific microbial banks and the growing interest among scientists in evaluating effects across diverse genotypes and environments, there is potential to refine the SynCom approach. This can ultimately provide farmers with a powerful tool applicable across various environmental settings (Jing et al., 2024). However, further studies are required to fully decipher SynCom-mediated responses and their persistence in inoculated plants across multiple seasons and environments as well as in diverse grapevine genotypes.

Funding

The authors thank the following projects for financial support: PRIMA – REVINE project (Italian MUR DM n.1966/2021, Project ID 20114–2), MicroBIO project (Funding ID: 2021.0072 - 51886) funded by Cariverona foundation, AGER 3 Project – Micro4Life (Grant n° 2022–2903) and CIRCOVINO project (founded by the Italian Ministry of Environment and Energy Security, EC-DEC n. 86 of 07 September 2023). This study was also conducted within the Agritech National Research Center and received funding from the European Union Next-Generation EU (PIANO NAZIONALE DI RIPRESA E RESILIENZA (PNRR)—MISSIONE 4 COMPONENTE 2, INVESTIMENTO 1.4—D.D. 1032 17/06/2022, CN00000022) and Shield4Grape project in the frame of Horizon Europe program (Grant agreement 101135088). This manuscript reflects only the authors' views and opinions, neither the European Union nor the European Commission can be considered responsible for them.

Data availability

16S sequences of the bacterial collection are deposited in NCBI under accessions OP994307-OP994344.

Metabarcoding data of bacterial (V3-V4 region of the 16S sequence) and fungal (ITS2 sequence) communities are deposited in NCBI under BioProject PRJNA1026525, BioSample SAMN37748419-SAMN37748424 and SRA objects SRR26363391-SRR26363395.

RNAseq data are deposited in NCBI under BioProject PRJNA1026525, BioSample SAMN37766153 and SAMN37766154 and SRA objects SRR26348056 and SRR26348055.

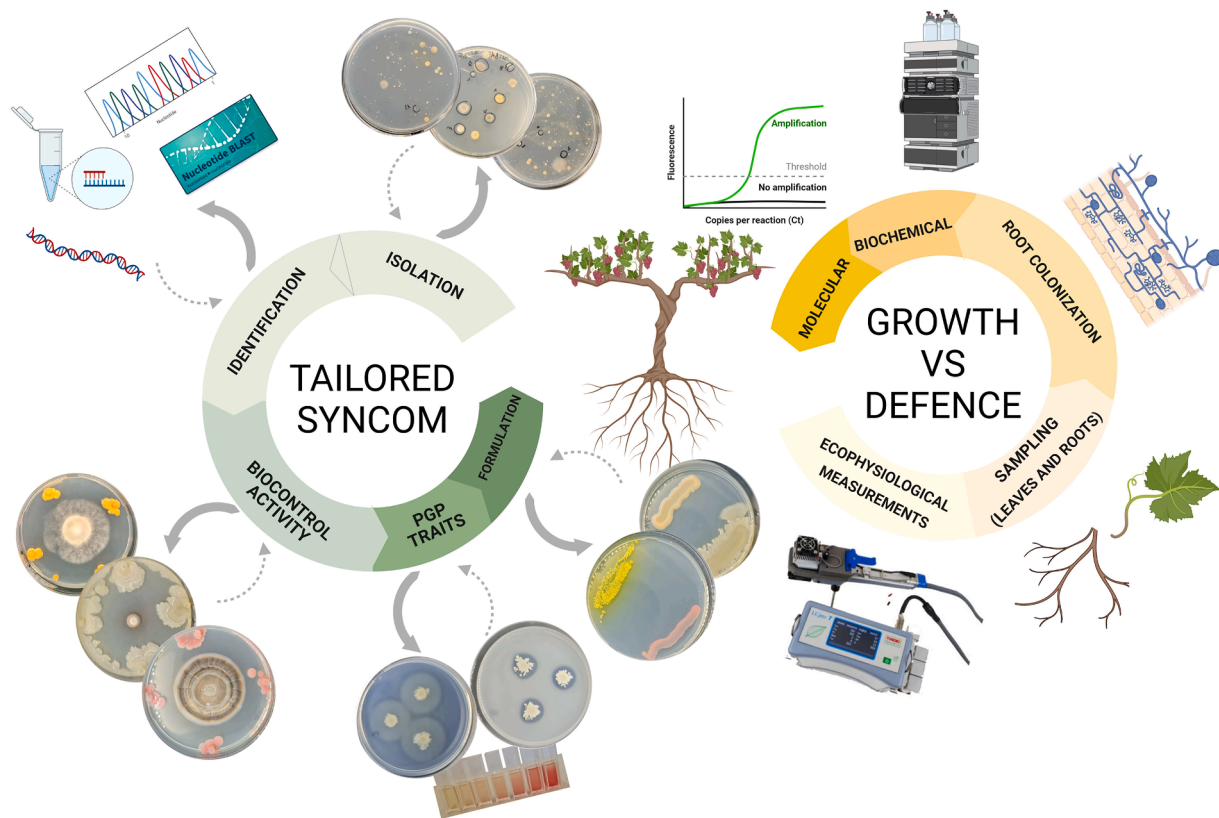


Fig. 6. Overview of the adopted holistic approach. To test the SynCom developed in this work, several specific features of each isolate (e.g., PGP traits, biocontrol activity, formulation characteristics, etc...) were considered and, once formulated, the holobiont responses were analyzed to decipher the impact on plant fitness. The experimental strategy followed physiological, biochemical and transcriptional rearrangements induced by the SynCom application to be observed.

ORCID iD authorship contribution statement

Marco Sandrini: Writing – original draft, Investigation, Formal analysis, Conceptualization. **Walter Chitarra:** Writing – review & editing, Writing – original draft, Supervision, Project administration, Investigation, Funding acquisition, Formal analysis, Data curation, Conceptualization. **Chiara Pagliarani:** Writing – review & editing, Methodology, Data curation. **Loredana Moffa:** Writing – review & editing, Formal analysis. **Maurizio Petrozziello:** Writing – review & editing, Formal analysis. **Paola Colla:** Writing – review & editing, Formal analysis. **Riccardo Velasco:** Writing – review & editing. **Raffaella Balestrini:** Writing – review & editing, Writing – original draft, Investigation, Formal analysis, Conceptualization. **Luca Nerva:** Writing – review & editing, Writing – original draft, Supervision, Project administration, Funding acquisition, Formal analysis, Data curation, Conceptualization.

Declaration of competing interest

The authors declare that they have no known competing financial interests or personal relationships that could have appeared to influence the work reported in this paper.

Acknowledgments

The authors are grateful to Dr. Giancarlo Babbo formerly employed by Sumitomo Chem Italia for kindly providing the MycoApply product used in this study. The authors thank Alison Garside for the manuscript English editing service.

Supplementary materials

Supplementary material associated with this article can be found, in the online version, at [doi:10.1016/j.stress.2024.100686](https://doi.org/10.1016/j.stress.2024.100686).

Data availability

Data will be made available on request.

References

- Abarenkov, K., Henrik Nilsson, R., Larsson, K., Alexander, I.J., Eberhardt, U., Erland, S., et al., 2010. The UNITE database for molecular identification of fungi—recent updates and future perspectives. *New Phytol.* 186, 281–285.
- Alagna, F., Balestrini, R., Chitarra, W., Marsico, A., Nerva, L., 2020. Getting ready with the priming: Innovative weapons against biotic and abiotic crop enemies in a global changing scenario. *Priming-Mediated Stress and Cross-Stress Tolerance in Crop Plants*. Elsevier, pp. 35–56.
- Armanhi, J.S.L., de Souza, R.S.C., Biazotti, B.B., Yassitepe, J.E., de, C.T., Arruda, P., 2021. Modulating drought stress response of maize by a synthetic bacterial community. *Front. Microbiol.* 3042.
- Armanhi, J.S.L., De Souza, R.S.C., Damasceno, N., de, B., De Araujo, L.M., Imperial, J., Arruda, P., 2018. A community-based culture collection for targeting novel plant growth-promoting bacteria from the sugarcane microbiome. *Front. Plant Sci.* 8, 317588.
- Armijo, G., Schlechter, R., Agurto, M., Muñoz, D., Nuñez, C., Arce-Johnson, P., 2016. Grapevine pathogenic microorganisms: understanding infection strategies and host response scenarios. *Front. Plant Sci.* 7, 382.
- Aziz, A., Verhagen, B., Magnin-Robert, M., Couderchet, M., Clément, C., Jeandet, P., Trotel-Aziz, P., 2016. Effectiveness of beneficial bacteria to promote systemic resistance of grapevine to gray mold as related to phytoalexin production in vineyards. *Plant Soil.* 405, 141–153.
- Balestrini, R., Brunetti, C., Chitarra, W., Nerva, L., 2020. Photosynthetic Traits and Nitrogen Uptake in Crops: Which Is the Role of Arbuscular Mycorrhizal Fungi? *Plants* 9, 1105.
- Balestrini, R., Salvioli, A., Dal Molin, A., Novero, M., Gabelli, G., Paparelli, E., et al., 2017. Impact of an arbuscular mycorrhizal fungus versus a mixed microbial inoculum on the transcriptome reprogramming of grapevine roots. *Mycorrhiza* 27, 417–430.

- Basile, B., Rouphael, Y., Colla, G., Soppelsa, S., Andreotti, C., 2020. Appraisal of emerging crop management opportunities in fruit trees, grapevines and berry crops facilitated by the application of biostimulants. *Sci Hort* 267, 109330.
- Belfiore, N., Nerva, L., Fasolini, R., Giotti, F., Lovat, L., Chitarra, W., 2021. Leaf gas exchange and abscisic acid in leaves of Glera grape variety during drought and recovery. *Theor. Exp. Plant Physiol.* 33, 261–270.
- Berendsen, R.L., Vismans, G., Yu, K., Song, Y., de Jonge, R., Burgman, W.P., et al., 2018. Disease-induced assemblage of a plant-beneficial bacterial consortium. *ISME J.* 12, 1496–1507.
- Bolyen, E., Rideout, J.R., Dillon, M.R., Bokulich, N.A., Abnet, C.C., Al-Ghalith, G.A., et al., 2019. Reproducible, interactive, scalable and extensible microbiome data science using QIIME 2. *Nat. Biotechnol.* 37, 852–857.
- Brotman, Y., Liseč, J., Meret, M., Chet, I., Willmitzer, L., Viterbo, A., 2012. Transcript and metabolite analysis of the *Trichoderma*-induced systemic resistance response to *Pseudomonas syringae* in *Arabidopsis thaliana*. *Microbiology* 158, 139–146.
- Burketova, L., Trda, L., Ott, P.G., Valentova, O., 2015. Bio-based resistance inducers for sustainable plant protection against pathogens. *Biotechnol. Adv.* 33, 994–1004.
- Callahan, B.J., McMurdie, P.J., Rosen, M.J., Han, A.W., Johnson, A.J.A., Holmes, S.P., 2016. DADA2: high-resolution sample inference from Illumina amplicon data. *Nat. Methods* 13, 581–583.
- Carlström, C.I., Field, C.M., Bortfeld-Miller, M., Müller, B., Sunagawa, S., Vorholt, J.A., 2019. Synthetic microbiota reveal priority effects and keystone strains in the *Arabidopsis* phyllosphere. *Nat. Ecol. Evol.* 3, 1445–1454.
- Carrión, V.J., Perez-Jaramillo, J., Cordovez, V., Tracanna, V., De Hollander, M., Ruiz-Buck, D., et al., 2019. Pathogen-induced activation of disease-resistance functions in the endophytic root microbiome. *Science* 366, 606–612.
- Chitarra, W., Cuzzo, D., Ferrandino, A., Secchi, F., Palmano, S., Perrone, I., et al., 2018. Dissecting interplays between *Vitis vinifera* L. and grapevine virus B (GVB) under field conditions. *Mol. Plant Pathol.* 19, 2651–2666.
- Chitarra, W., Pagliarini, C., Maserti, B., Lumini, E., Siciliano, I., Cascone, P., et al., 2016. Insights on the impact of arbuscular mycorrhizal symbiosis on tomato tolerance to water stress. *Plant Physiol.* 171, 1009–1023.
- Chitarra, W., Siciliano, I., Ferrocino, I., Gullino, M.L., Garibaldi, A., 2015. Effect of elevated atmospheric CO₂ and temperature on the disease severity of rocket plants caused by *Fusarium* wilt under phytotron conditions. *PLoS One* 10, e0140769.
- Cole, J.R., Wang, Q., Fish, J.A., Chai, B., McGarrell, D.M., Sun, Y., et al., 2014. Ribosomal Database Project: data and tools for high throughput rRNA analysis. *Nucleic Acids Res.* 42, D633–D642.
- Corwin, D.L., 2021. Climate change impacts on soil salinity in agricultural areas. *Eur. J. Soil Sci.* 72, 842–862.
- Cregger, M., Veach, A., Yang, Z., Crouch, M., Vilgalys, R., Tuskan, G., Schadt, C., 2018. The Populus holobiont: dissecting the effects of plant niches and genotype on the microbiome. *Microbiome* 6, 1–14.
- Dobin, A., Davis, C.A., Schlesinger, F., Drenkow, J., Zaleski, C., Jha, S., et al., 2013. STAR: ultrafast universal RNA-seq aligner. *Bioinformatics* 29, 15–21.
- Faust, K., Raes, J., 2012. Microbial interactions: from networks to models. *Nat. Rev. Microbiol.* 10, 538–550.
- Faust, K., Raes, J., 2016. CoNet app: inference of biological association networks using Cytoscape. *F1000Research* 5.
- Fiorilli, V., Martínez-Medina, A., Pozo, M.J., Lanfranco, L., 2024. Plant immunity modulation in arbuscular mycorrhizal symbiosis and its impact on pathogens and pests. *Annu Rev. Phytopathol.* 62, 127–156.
- Gambetta, G.A., Herrera, J.C., Dayer, S., Feng, Q., Hochberg, U., Castellarin, S.D., 2020. The physiology of drought stress in grapevine: towards an integrative definition of drought tolerance. *J. Exp. Bot.* 71, 4658–4676.
- Geetha, K., Venkatesham, E., Hindumathi, A., Bhadrarai, B., 2014. Isolation, screening and characterization of plant growth promoting bacteria and their effect on *Vigna Radita* (L.) R. Wilczek. *Int J Curr Microbiol Appl Sci* 3, 799–899.
- Giudice, G., Moffa, L., Niero, M., Duso, C., Sandrini, M., Vazzoler, L.F., et al., 2022. Novel sustainable strategies to control *Plasmodium viticola* in grapevine unveil new insights on priming responses and arthropods ecology. *Pest. Manage Sci.* 78, 2342–2356.
- Giudice, G., Moffa, L., Varotto, S., Cardone, M.F., Bergamini, C., De Lorenzis, G., et al., 2021. Novel and emerging biotechnological crop protection approaches. *Plant Biotechnol. J.* 19, 1495–1510.
- Gopalakrishnan, S., Vadlamudi, S., Bandikinda, P., Sathya, A., Vijayabharathi, R., Rupela, O., et al., 2014. Evaluation of *Streptomyces* strains isolated from herbal vermicompost for their plant growth-promotion traits in rice. *Microbiol. Res.* 169, 40–48.
- Grimplet, J., Van Hemert, J., Carbonell-Bejerano, P., Díaz-Riquelme, J., Dickerson, J., Fennell, A., et al., 2012. Comparative analysis of grapevine whole-genome gene predictions, functional annotation, categorization and integration of the predicted gene sequences. *BMC Res. Notes* 5, 213.
- Guerrieri, M.C., Fanfoni, E., Fiorini, A., Trevisan, M., Puglisi, E., 2020. Isolation and screening of extracellular GPPR from the rhizosphere of tomato plants after long-term reduced tillage and cover crops. *Plants* 9, 668.
- Gul, N., Wani, I.A., Mir, R.A., Nowshehri, J.A., Aslam, S., Gupta, R., et al., 2023. Plant growth promoting microorganisms mediated abiotic stress tolerance in crop plants: a critical appraisal. *Plant Growth Regul.* 100, 7–24.
- Guo, Y., Luo, H., Wang, L., Xu, M., Wan, Y., Chou, M., et al., 2021. Multifunctionality and microbial communities in agricultural soils regulate the dynamics of a soil-borne pathogen. *Plant Soil.* 461, 309–322.
- Huang, Z., Wang, Z., Shi, B., Wei, D., Chen, J., Wang, S., Gao, B., 2015. Simultaneous determination of salicylic acid, jasmonic acid, methyl salicylate, and methyl jasmonate from *Ulmus pumila* leaves by GC-MS. *Int. J. Anal. Chem.* 2015, 698630.
- Jeandet, P., Douillet-Breuil, A.-C., Bessis, R., Debord, S., Sbaghi, M., Adrian, M., 2002. Phytoalexins from the *Vitaceae*: biosynthesis, phytoalexin gene expression in transgenic plants, antifungal activity, and metabolism. *J. Agric. Food Chem.* 50, 2731–2741.
- Jiang, Y., Li, Q., Chen, X., Jiang, C., 2016. Isolation and cultivation methods of Actinobacteria. *Actinobacteria—Basics Biotechnol Appl* 39–57.
- Jing, J., Garbeva, P., Raaijmakers, J.M., Medema, M.H., 2024. Strategies for tailoring functional microbial synthetic communities. *ISMe J.* 18, wrae049.
- Jurburg, S.D., Eisenhauer, N., Buscot, F., Chatzinotas, A., Chaudhari, N.M., Heintz-Buschart, A., et al., 2022. Potential of microbiome-based solutions for agrifood systems. *Nat. Food* 3, 557–560.
- Kaur, S., Egidio, E., Qiu, Z., Macdonald, C.A., Verma, J.P., Trivedi, P., et al., 2022. Synthetic community improves crop performance and alters rhizosphere microbial communities. *J. Sustain Agric Environ* 1, 118–131.
- Kavya, T., Govindasamy, V., Suman, A., Abraham, G., 2024. Plant-Actinobacteria interactions for biotic and abiotic stress management in crops. *Plant Holobiont Engineering For Climate-Smart Agriculture*. Springer Nature Singapore, Singapore, pp. 441–463.
- Keller, M., 2020. *The Science of Grapevines*. Academic pressElsevier.
- Khandani, Y., Sarikhani, H., Gholami, M., Rad, A.C., Yousefi, S., Sodini, M., et al., 2024. Exogenous auxin improves the growth of grapevine (*Vitis vinifera* L.) under drought stress by mediating physiological, biochemical and hormonal modifications. *J. Soil Sci Plant Nut* 24, 3422–3440.
- Kokare, C., Mahadik, K., Kadam, S., Chopade, B., 2004. Isolation, characterization and antimicrobial activity of marine halophilic *Actinopolyspora* species AH1 from the west coast of India. *Curr. Sci.* 593–597.
- Lebeis, S.L., 2015. Greater than the sum of their parts: characterizing plant microbiomes at the community-level. *Curr. Opin. Plant Biol.* 24, 82–86.
- Li, Z., Bai, X., Jiao, S., Li, Y., Li, P., Yang, Y., et al., 2021. A simplified synthetic community rescues *Astragalus mongholicus* from root rot disease by activating plant-induced systemic resistance. *Microbiome* 9, 1–20.
- Li, Z., Chang, S., Lin, L., Li, Y., An, Q., 2011. A colorimetric assay of 1-aminocyclopropane-1-carboxylate (ACC) based on ninhydrin reaction for rapid screening of bacteria containing ACC deaminase. *Lett. Appl. Microbiol.* 53, 178–185.
- Liao, Y., Smyth, G.K., Shi, W., 2014. featureCounts: an efficient general purpose program for assigning sequence reads to genomic features. *Bioinformatics* 30, 923–930.
- Liu, H., Brettell, L.E., Qiu, Z., Singh, B.K., 2020. Microbiome-mediated stress resistance in plants. *Trends. Plant Sci.* 25, 733–743.
- Liu, H., Qiu, Z., Ye, J., Verma, J.P., Li, J., Singh, B.K., 2022. Effective colonisation by a bacterial synthetic community promotes plant growth and alters soil microbial community. *J. Sustain Agric Environ* 1, 30–42.
- Liu, Y.-X., Qin, Y., Bai, Y., 2019. Reductionist synthetic community approaches in root microbiome research. *Curr. Opin. Microbiol.* 49, 97–102.
- Livak, K.J., Schmittgen, T.D., 2001. Analysis of relative gene expression data using real-time quantitative PCR and the 2⁻ΔΔCT method. *Methods* 25, 402–408.
- Louden, B.C., Haarmann, D., Lynne, A.M., 2011. Use of blue agar CAS assay for siderophore detection. *J. Microbiol. Biol. Educ.* 12, 51–53.
- Lundberg, D.S., Youtstone, S., Mieczkowski, P., Jones, C.D., Dangel, J.L., 2013. Practical innovations for high-throughput amplicon sequencing. *Nat. Methods* 10, 999–1002.
- Magoč, T., Salzberg, S.L., 2011. FLASH: fast length adjustment of short reads to improve genome assemblies. *Bioinformatics* 27, 2957–2963.
- Minio, A., Cantu, D., 2022. Grapegenomics.com: a web portal with genomic data and analysis tools for wild and cultivated grapevines. *Zenodo*. <https://doi.org/10.5281/zenodo.10570120>.
- Nerva, L., García, J., Favaretto, F., Giudice, G., Moffa, L., Sandrini, M., et al., 2022a. The hidden world within plants: metatranscriptomics unveils the complexity of wood microbiomes. *J. Exp. Bot.* 73, 2682–2697.
- Nerva, L., Balestrini, R., Chitarra, W., 2023. From plant nursery to field: persistence of mycorrhizal symbiosis balancing effects on growth-defence tradeoffs mediated by rootstock. *Agronomy* 13, 229.
- Nerva, L., Giudice, G., Quiroga, G., Belfiore, N., Lovat, L., Perria, R., et al., 2022b. Mycorrhizal symbiosis balances rootstock-mediated growth-defence tradeoffs. *Biol. Fertil. Soils.* 58, 17–34.
- Nerva, L., Guaschino, M., Pagliarini, C., De Rosso, M., Lovisolo, C., Chitarra, W., 2022c. Spray induced gene silencing targeting a *glutathione S-transferase* gene improves resilience to drought in grapevine. *Plant Cell Environ.* 45, 347–361.
- Nerva, L., Moffa, L., Giudice, G., Giorgianni, A., Tomasi, D., Chitarra, W., 2021. Microscale analysis of soil characteristics and microbiomes reveals potential impacts on plants and fruit: vineyard as a model case study. *Plant Soil.* 462, 525–541.
- Nerva, L., Pagliarini, C., Pugliese, M., Monchiero, M., Gonthier, S., Gullino, M.L., et al., 2019. Grapevine Phyllosphere Community Analysis in Response to Elicitor Application against Powdery Mildew. *Microorganisms* 7, 662.
- Nerva, L., Sandrini, M., Moffa, L., Velasco, R., Balestrini, R., Chitarra, W., 2022d. Breeding toward improved ecological plant-microbiome interactions. *Trends. Plant Sci.* 27, 1134–1143.
- Oh, M.-M., Trick, H.N., Rajashekar, C., 2009. Secondary metabolism and antioxidants are involved in environmental adaptation and stress tolerance in lettuce. *J. Plant Physiol.* 166, 180–191.
- Oukala, N., Pastor-Fernández, J., Sanmartín, N., Aissat, K., Pastor, V., 2021. Endophytic bacteria from the sahara desert protect tomato plants against *Botrytis cinerea* under different experimental conditions. *Curr. Microbiol.* 78, 2367–2379.
- Prigigallo, M.I., Staropoli, A., Vinalé, F., Bubici, G., 2023. Interactions between plant-beneficial microorganisms in a consortium: *Streptomyces microflavus* and *Trichoderma harzianum*. *Microb. Biotechnol.* 16, 2292–2312.
- Qiu, Z., Egidio, E., Liu, H., Kaur, S., Singh, B.K., 2019. New frontiers in agriculture productivity: optimised microbial inoculants and *in situ* microbiome engineering. *Biotechnol. Adv.* 37, 107371.

- Quast, C., Pruesse, E., Yilmaz, P., Gerken, J., Schweer, T., Yarza, P., et al., 2012. The SILVA ribosomal RNA gene database project: improved data processing and web-based tools. *Nucleic. Acids. Res.* 41, D590–D596.
- Ristaino, J.B., Anderson, P.K., Bebber, D.P., Brauman, K.A., Cunniffe, N.J., Fedoroff, N. V., et al., 2021. The persistent threat of emerging plant disease pandemics to global food security. *Proc. Natl. Acad. Sci.* 118, e2022239118.
- Rivers, A.R., Weber, K.C., Gardner, T.G., Liu, S., Armstrong, S.D., 2018. ITSxpress: software to rapidly trim internally transcribed spacer sequences with quality scores for marker gene analysis. *F1000Research* 7.
- Sandrini, M., Moffa, L., Velasco, R., Balestrini, R., Chitarra, W., Nerva, L., 2022a. Microbe-assisted crop improvement: a sustainable weapon to restore holobiont functionality and resilience. *Hortic. Res.* 9, uhac160.
- Sandrini, M., Nerva, L., Sillo, F., Balestrini, R., Chitarra, W., Zampieri, E., 2022b. Abiotic stress and belowground microbiome: The potential of omics approaches. *Int. J. Mol. Sci.* 23, 1091.
- Singh, T.B., Sahai, V., Ali, A., Prasad, M., Yadav, A., Shrivastav, P., et al., 2020. Screening and evaluation of PGPR strains having multiple PGP traits from hilly terrain. *J. Appl. Biol. Biotechnol.* 8, 38–44.
- Toju, H., Peay, K.G., Yamamichi, M., Narisawa, K., Hiruma, K., Naito, K., et al., 2018. Core microbiomes for sustainable agroecosystems. *Nat. Plants.* 4, 247–257.
- Trivedi, P., Leach, J.E., Tringe, S.G., Sa, T., Singh, B.K., 2020. Plant–microbiome interactions: from community assembly to plant health. *Nat. Rev. Microbiol.* 18, 607–621.
- Trouvelot, A., Kough, J., Gianinazzi-Pearson, V., 1986. Estimation of Vesicular Arbuscular Mycorrhizal Infection levels. *Research for Methods Having a Functional Significance.* Institut national de le recherche agronomique, Paris, p. c1986.
- Vandenkoornhuysse, P., Quaiser, A., Duhamel, M., Le Van, A., Dufresne, A., 2015. The importance of the microbiome of the plant holobiont. *New. Phytol.* 206, 1196–1206.
- van Huylenbroeck, J.M., van Laere, I.M., Piqueras, A., Debergh, P.C., Bueno, P., 1998. Time course of catalase and superoxide dismutase during acclimatization and growth of micropropagated *Calathea* and *Spathiphyllum* plants. *Plant Growth Regul.* 26, 7–14.
- van Leeuwen, C., Sgubin, G., Bois, B., Ollat, N., Swingedouw, D., Zito, S., et al., 2024. Climate change impacts and adaptations of wine production. *Nat. Rev. Earth. Environ.* 5, 258–275.
- Veach, A.M., Morris, R., Yip, D.Z., Yang, Z.K., Engle, N.L., Cregger, M.A., et al., 2019. Rhizosphere microbiomes diverge among *Populus trichocarpa* plant-host genotypes and chemotypes, but it depends on soil origin. *Microbiome* 7, 1–15.
- Verhagen, B.W., Glazebrook, J., Zhu, T., Chang, H.-S., Van Loon, L., Pieterse, C.M., 2004. The transcriptome of rhizobacteria-induced systemic resistance in *Arabidopsis*. *Mol. Plant Microbe Interact.* 17, 895–908.
- Verhagen, B.W., Trotel-Aziz, P., Couderchet, M., Höfte, M., Aziz, A., 2010. *Pseudomonas* spp.-induced systemic resistance to *Botrytis cinerea* is associated with induction and priming of defence responses in grapevine. *J. Exp. Bot.* 61, 249–260.
- Wei, Y., Wu, Y., Yan, Y., Zou, W., Xue, J., Ma, W., et al., 2018. High-throughput sequencing of microbial community diversity in soil, grapes, leaves, grape juice and wine of grapevine from China. *PLoS. One* 13, e0193097.
- Williams, A., de Vries, F.T., 2020. Plant root exudation under drought: implications for ecosystem functioning. *New. Phytol.* 225, 1899–1905.
- Yu, K., Pieterse, C.M., Bakker, P.A., Berendsen, R.L., 2019. Beneficial microbes going underground of root immunity. *Plant Cell Environ.* 42, 2860–2870.
- Zou, Y., Xue, W., Luo, G., Deng, Z., Qin, P., Guo, R., et al., 2019. 1,520 reference genomes from cultivated human gut bacteria enable functional microbiome analyses. *Nat. Biotechnol.* 37, 179–185.